Electronic Supplementary Material (ESI) for Journal of Materials Chemistry A.

A stable metal cluster-metalloporphyrin MOF with high capacity for cationic dye removal

Zheng Wang,[ab] Jian-Hua Zhang,[a] Ji-Jun Jiang,[a] Hai-Ping Wang,[a] Zhang-Wen Wei,[a] Xunjin Zhu,*[b] Mei Pan,*[a] and Cheng-Yong Su[a]

[a]*Lehn Institute of Functional materials, MOE Laboratory of Bioinorganic and Synthetic Chemistry, School of Chemistry, Sun Yat-Sen University, Guangzhou 510275, China.*

[b]*Department of Chemistry, Hong Kong Baptist University, Waterloo Road, Kowloon Tong, Hong Kong, China.*

1. Crystal structure of LIFM-WZ-3

Table S1. Crystal data and structure refinement for LIFM-WZ-3

Identification code	LIFM-WZ-3
Empirical formula	$C_{96}H_{48}Cl_2Cu_{4.50}N_{40}O_{0.50}$
Formula weight	2126.57
Temperature	100 K
Wavelength	1.54178Å
Crystal system	Monoclinic
Space group	*P2/m*
a, Å	16.9552(10)
b, Å	19.4089(10)
c, Å	18.5986(9)
α, °	90
β, °	99.771(4)
γ, °	90
V, Å^3	6031.7(6)
Z	2
Calculated density	1.171
Crystal size, mm	0.11 x 0.10 x 0.09
Absorption coefficient	1.752
F(000)	2145
Theta range for data collection	2.28 to 52.99°
Limiting indices	-17<=h<=17, 0<=k<=19, 0<=l<=19
Reflections collected	7180
Independent reflections	7180 [R(int) = 0.0997]
Completeness to theta = 65.54	98.3%
Refinement method	Full-matrix least-res on F^2
Data/restraints/parameters	7180/1924/956
Quality-of-fit indicator	1.051
Final *R* indices [*I*>2σ(*I*)]	$R_1 = 0.1360$ $_wR_2 = 0.2756$
R indices (all data)	$R_1 = 0.1904$ $_wR_2 = 0.2927$
Largest diff. peak and hole	1.327 and -0.855 e.Å^{-3}

Table S2. Selected bond lengths (Å) and angles (deg) for LIFM-WZ-3

LIFM-WZ-3			
O(1W)-Cu(3)	2.343(5)	Cu(2)-Cl(2)#7	2.562(9)
O(1W)-Cu(3)#1	2.343(5)	Cu(2)-Cl(2)	2.562(9)
Cu(1)-N(3)	1.975(19)	Cu(3)-N(10)#8	1.922(18)
Cu(1)-N(2)#2	1.997(11)	Cu(3)-N(10)	1.922(18)
Cu(1)-N(2)	1.997(11)	Cu(3)-Cl(1)	2.571(14)
Cu(1)-N(1)	1.999(18)	Cu(4)-N(9)	1.938(16)
Cu(2)-N(6)#3	1.965(12)	Cu(4)-N(9)#8	1.938(16)
Cu(2)-N(6)#4	1.965(11)	Cu(4)-N(5)#5	1.974(13)
Cu(2)-N(6)#5	1.965(11)	Cu(4)-N(5)#6	1.974(13)
Cu(2)-N(6)#6	1.965(11)	Cu(4)-Cl(2)	2.571(11)
Cu(5)-N(13A)#8	2.034(17)	Cu(4)-Cl(1)	2.610(13)
Cu(5)-N(12)	2.034(16)	Cu(5)-N(13A)	2.034(17)
Cu(5)-N(12)#8	2.034(16)	Cu(5)-N(12A)	2.042(16)
Cu(5)-N(12A)#8	2.042(16)	Cu(5)-N(13)#8	2.049(17)
Cu(5)-N(13)	2.049(17)	N(5)-Cu(4)#9	1.974(13)
N(6)-Cu(2)#9	1.965(11)		
N(3)-Cu(1)-N(2)#2	89.3(4)	N(6)#3-Cu(2)-N(6)#4	90.3(6)
N(3)-Cu(1)-N(2)	89.3(4)	N(6)#3-Cu(2)-N(6)#5	180.000(3)
N(2)#2-Cu(1)-N(2)	178.3(7)	N(6)#4-Cu(2)-N(6)#5	89.7(7)
N(3)-Cu(1)-N(1)	179.8(7)	N(6)#3-Cu(2)-N(6)#6	89.7(6)
N(2)#2-Cu(1)-N(1)	90.7(4)	N(6)#4-Cu(2)-N(6)#6	180.000(4)
N(2)-Cu(1)-N(1)	90.7(4)	N(6)#5-Cu(2)-N(6)#6	90.3(6)
N(6)#3-Cu(2)-Cl(2)#7	86.0(4)	N(6)#3-Cu(2)-Cl(2)	94.0(4)
N(6)#4-Cu(2)-Cl(2)#7	86.0(4)	N(6)#4-Cu(2)-Cl(2)	94.0(4)
N(6)#5-Cu(2)-Cl(2)#7	94.0(4)	N(6)#5-Cu(2)-Cl(2)	86.0(4)
N(6)#6-Cu(2)-Cl(2)#7	94.0(4)	N(6)#6-Cu(2)-Cl(2)	86.0(4)
O(1W)-Cu(3)-Cl(1)	123.8(4)	Cl(2)#7-Cu(2)-Cl(2)	180.000(2)
N(9)-Cu(4)-N(9)#8	90.4(9)	N(10)#8-Cu(3)-N(10)	92.5(10)
N(9)-Cu(4)-N(5)#5	90.3(6)	N(10)#8-Cu(3)-O(1W)	126.2(6)
N(9)#8-Cu(4)-N(5)#5	176.7(7)	N(10)-Cu(3)-O(1W)	126.2(5)
N(9)-Cu(4)-N(5)#6	176.7(7)	N(10)#8-Cu(3)-Cl(1)	88.3(6)
N(9)#8-Cu(4)-N(5)#6	90.3(5)	N(5)#5-Cu(4)-Cl(1)	90.5(4)
N(5)#5-Cu(4)-N(5)#6	88.8(7)	N(5)#6-Cu(4)-Cl(1)	90.5(4)
N(9)-Cu(4)-Cl(2)	95.6(6)	Cl(2)-Cu(4)-Cl(1)	177.3(4)
N(9)#8-Cu(4)-Cl(2)	95.6(6)	N(13A)-Cu(5)-N(13A)#8	112.7(11)
N(5)#5-Cu(4)-Cl(2)	87.6(4)	N(13A)-Cu(5)-N(12)	89.6(8)
N(5)#6-Cu(4)-Cl(2)	87.6(4)	N(13A)#8-Cu(5)-N(12)	23.1(7)
N(9)-Cu(4)-Cl(1)	86.3(6)	N(13A)-Cu(5)-N(12)#8	23.1(7)
N(9)#8-Cu(4)-Cl(1)	86.3(6)	N(13A)#8-Cu(5)-N(12)#8	89.6(8)
N(12)-Cu(5)-N(12A)	179.4(10)	N(12)-Cu(5)-N(12)#8	66.4(11)
N(12)#8-Cu(5)-N(12A)	114.0(8)	N(13A)-Cu(5)-N(12A)#8	156.4(8)

N(12A)#8-Cu(5)-N(12A)	65.6(11)	N(13A)#8-Cu(5)-N(12A)#8	90.9(8)
N(13A)-Cu(5)-N(13)#8	65.0(8)	N(12)-Cu(5)-N(12A)#8	114.0(8)
N(13A)#8-Cu(5)-N(13)#8	176.3(9)	N(12)#8-Cu(5)-N(12A)#8	179.4(10)
N(12)-Cu(5)-N(13)#8	154.5(8)	N(13A)-Cu(5)-N(12A)	90.9(8)
N(12)#8-Cu(5)-N(13)#8	88.1(8)	N(13A)#8-Cu(5)-N(12A)	156.4(8)
N(12A)#8-Cu(5)-N(13)#8	91.5(9)	N(12)#8-Cu(5)-N(13)	154.5(8)
N(12A)-Cu(5)-N(13)#8	26.0(7)	N(12A)#8-Cu(5)-N(13)	26.0(7)
N(13A)-Cu(5)-N(13)	176.3(9)	N(12A)-Cu(5)-N(13)	91.5(9)
N(13A)#8-Cu(5)-N(13)	65.0(8)	N(13)#8-Cu(5)-N(13)	117.2(11)
N(12)-Cu(5)-N(13)	88.1(8)		

Symmetry transformations used to generate equivalent atoms:

#1 -x-4,-y+1,-z-3 #2 x,-y+2,z #3 -x-5,-y+1,-z-4 #4 -x-5,y,-z-4 #5 x+1,y,z #6 x+1,-y+1,z #7 -x-4,-y+1,-z-4 #8 x,-y+1,z #9 x-1,y,z

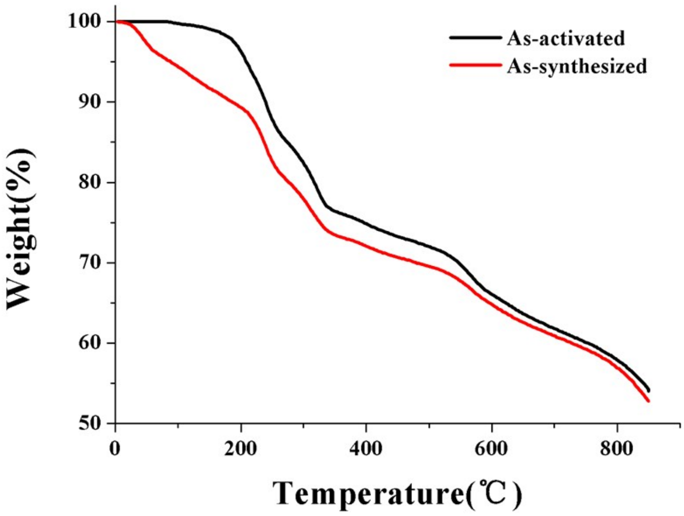

Fig. S1 TGA curves of LIFM-WZ-3.

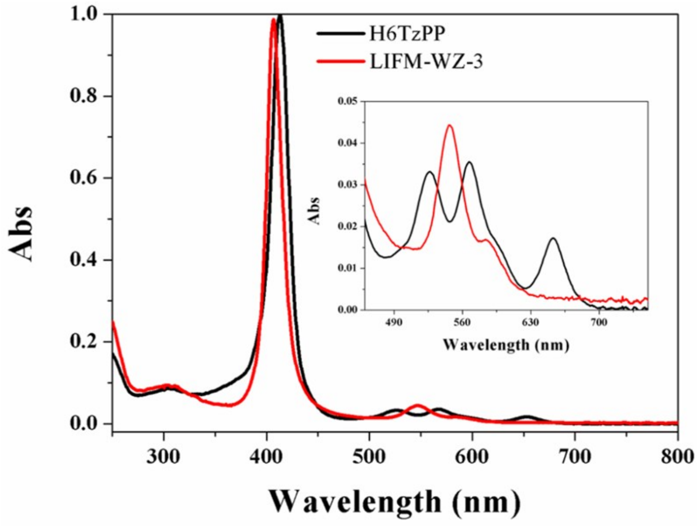

Fig. S2 The absorption spectra (NaOH/H_2O, 1×10^{-5} mol l^{-1}) of H_6TzPP and LIFM-WZ-3.

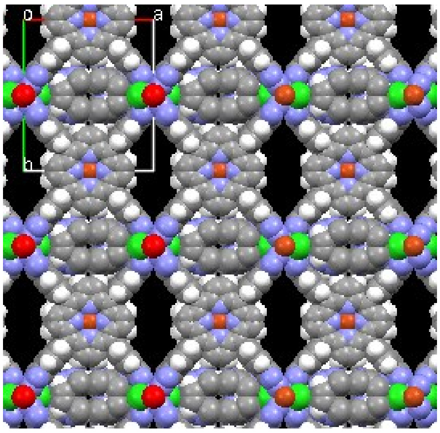

Fig. S3 Spindle-like 1D channels of LIFM-WZ-3 framework along *c* axis manifested in spacefill style.

2. Organic dyes with different sizes and charges

Table S3. Organic dyes with different sizes and charges

	Neutral			Anionic		Cationic			
Name	DY	SD-I	SD-II	AO$^-$	MO$^-$	MB$^+$	CV$^+$	BR$^+$	RB$^+$
	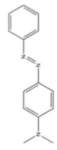	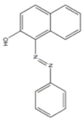	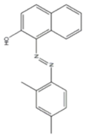	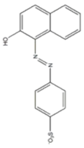	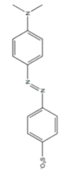	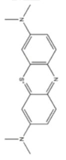	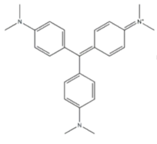	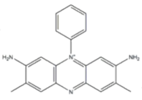	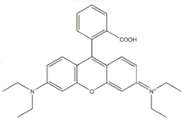
Charge	0	0	0	-1	-1	+1	+1	+1	+1
x(Å)	4.02	3.68	3.79	5.46	5.31	4.00	4.00	4.99	6.79
y(Å)	6.76	9.74	9.82	9.76	7.25	7.93	12.97	9.40	11.80
z(Å)	14.21	13.55	13.98	15.62	17.39	16.34	13.74	11.39	15.68

DY: dimethyl yellow; SD-I: Sudan-I; SD-II:Sudan-II; AO: Acid orange; MO: methyl orange; MB: methylene blue; CV: crystal violet; BR: basic red; RB: rhodamine B;

3. The nitrogen sorption isotherms at 77 K and pore size distribution

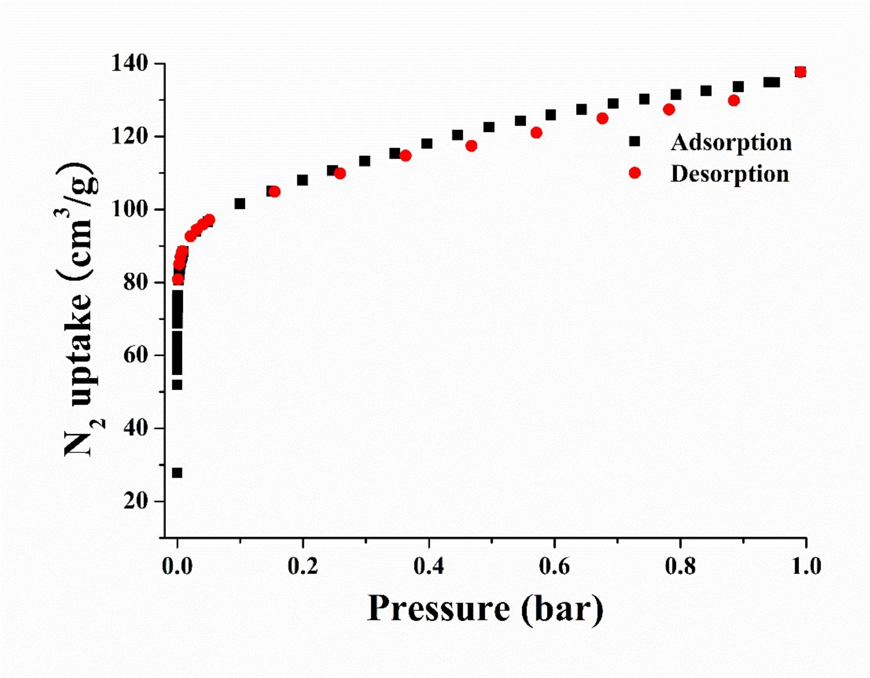

Fig. S4 N_2 sorption isotherm of LIFM-WZ-3 at 77 K.

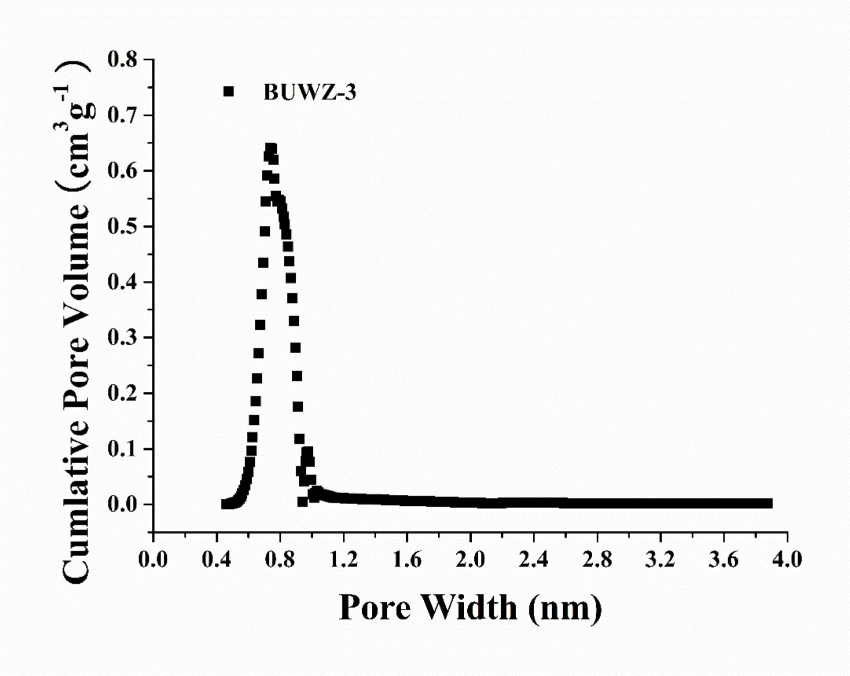

Fig. S5 Pore size distribution analyzed with SF method.

4. The sorption isotherms of CO_2, CH_4, C_2H_6, C_2H_4, C_3H_6 and water vapor

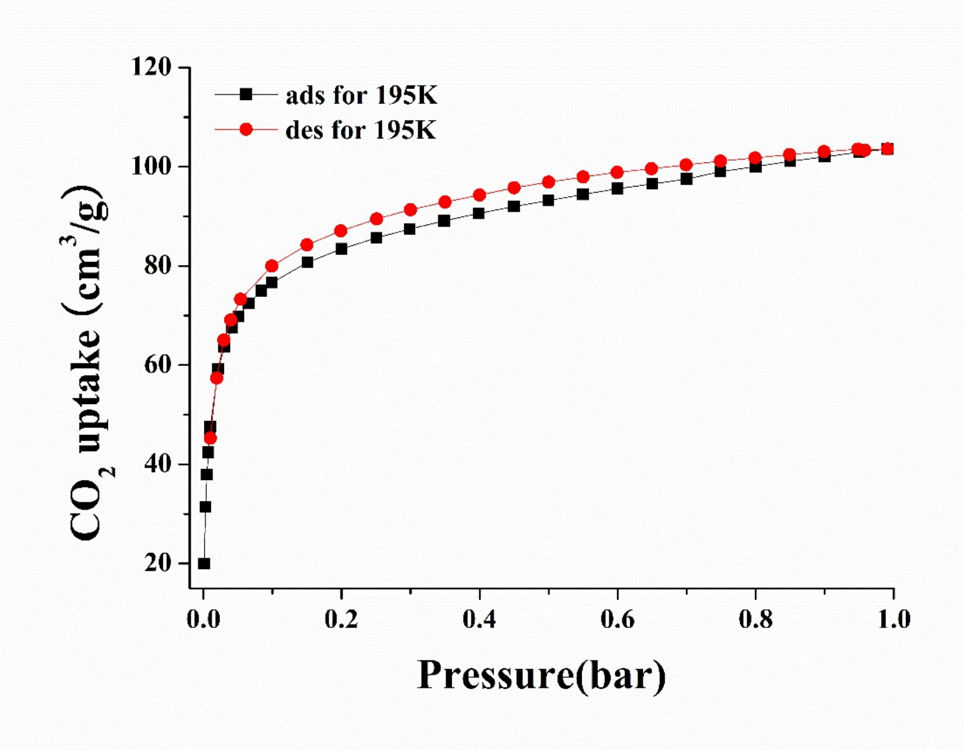

Fig. S6 CO_2 sorption isotherm of LIFM-WZ-3 at 195 K.

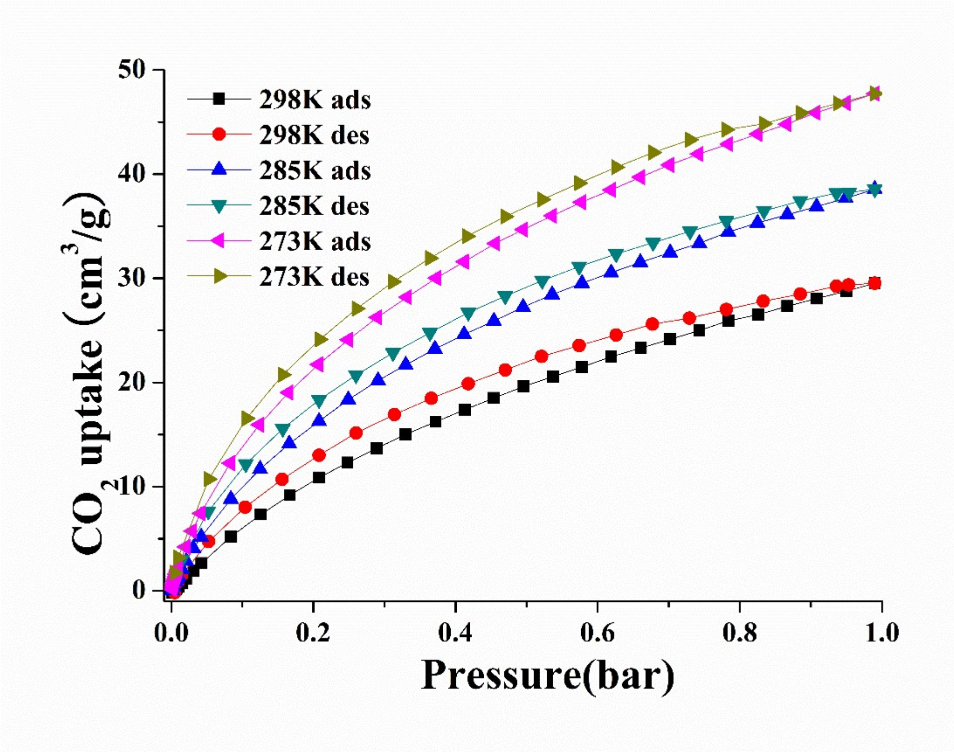

Fig. S7 CO_2 sorption isotherms of LIFM-WZ-3 at 298, 285 and 273 K.

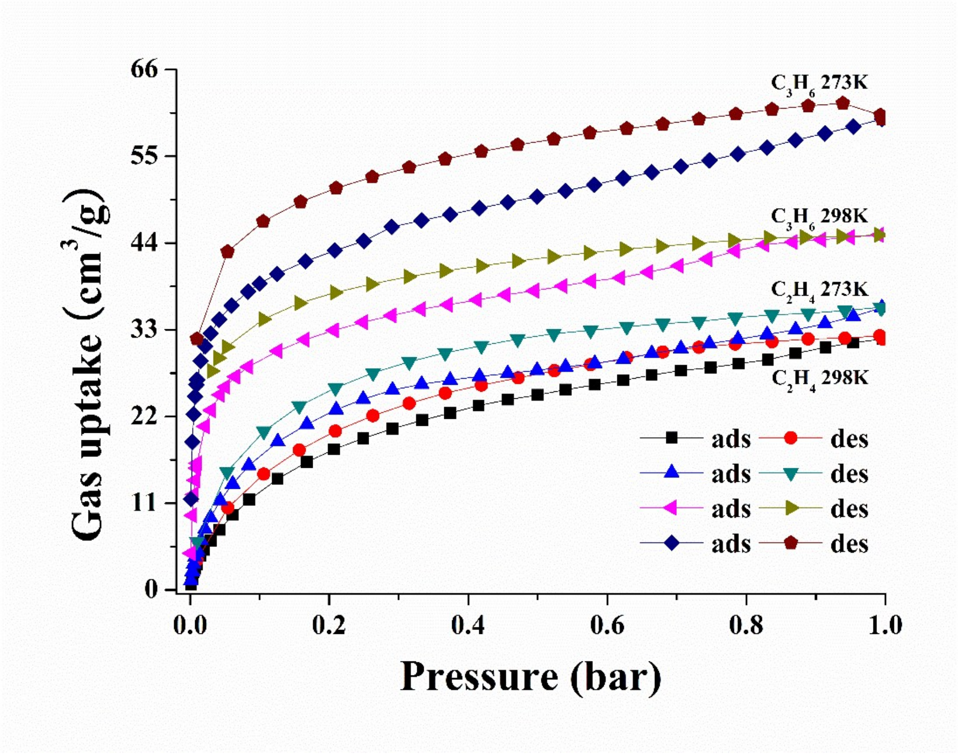

Fig. S8 C_2H_4 and C_3H_6 sorption isotherms of LIFM-WZ-3 at 298 and 273K.

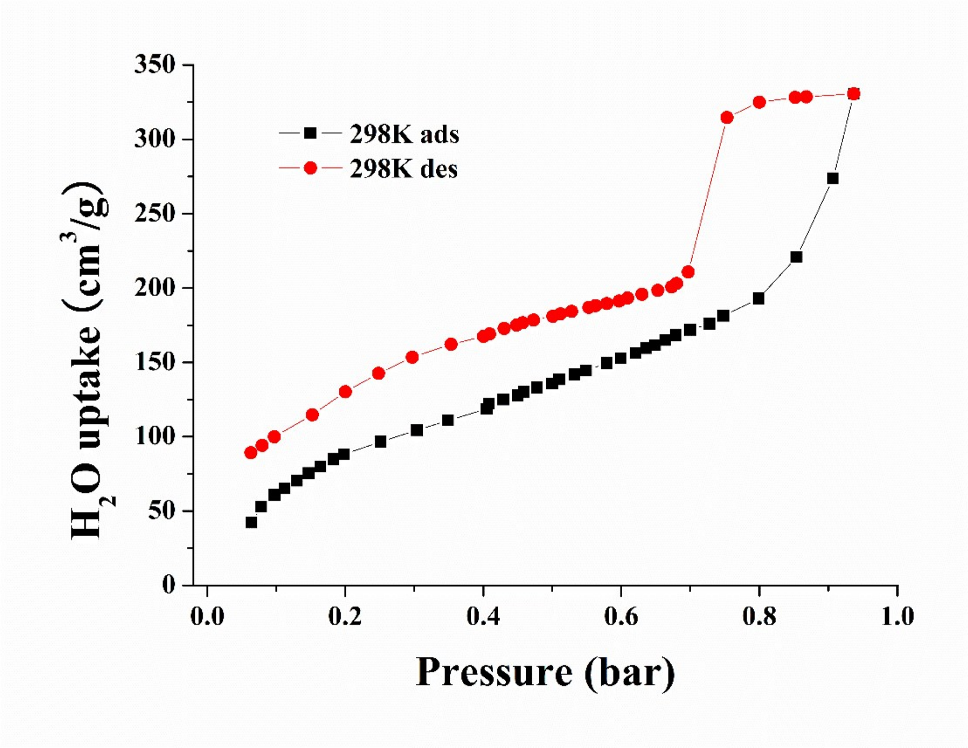

Fig. S9 Water vapor sorption isotherms of LIFM-WZ-3 at 298 K.

5. Calculations of adsorption isosteric heats

The isosteric heats of CO_2 for LIFM-WZ-3 were calculated with adsorption data measured at 298 and 273 K by the virial fitting method. A virial-type expression (eq. 1) which is composed of parameters a_i and b_i is used. In eq. 1, P is the pressure in torr, N is the adsorbed amount in mmol·g^{-1}, T is the temperature in Kelvin, a_i and b_i are the virial coefficients which are independent of temperature, and m and n are the numbers of coefficients required to adequately describe the isotherms. The values of the virial coefficients a_0 through a_m were then applied to calculate the isosteric heat of adsorption (eq 2). In eq. 2, Q_{st} is the coverage-dependent isosteric heat of adsorption and R is the universal gas constant.

$$\ln P = \ln \mathrm{N} + \frac{1}{\mathrm{T}} \sum_{\mathrm{i}=0}^{\mathrm{m}} \mathrm{a_i} \, \mathrm{N^i} + \sum_{\mathrm{i}=0}^{\mathrm{n}} \mathrm{b_i} \, \mathrm{N^i} \qquad \text{eq. 1}$$

$$\mathrm{Q_{st}} = -\mathrm{R} \sum_{\mathrm{i}=0}^{\mathrm{m}} \mathrm{a_i} \, \mathrm{N^i} \qquad \text{eq. 2}$$

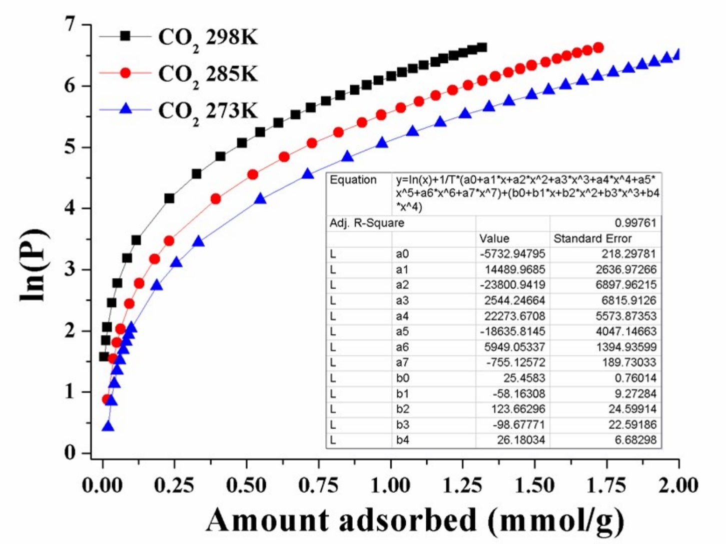

Equation	y=ln(x)+1/T*(a0+a1*x+a2*x^2+a3*x^3+a4*x^4+a5*x^5+a6*x^6+a7*x^7)+(b0+b1*x+b2*x^2+b3*x^3+b4*x^4)		
Adj. R-Square			0.99761
		Value	Standard Error
L	a0	-5732.94795	218.29781
L	a1	14489.9685	2636.97266
L	a2	-23800.9419	6897.96215
L	a3	2544.24664	6815.9126
L	a4	22273.6708	5573.87353
L	a5	-18635.8145	4047.14663
L	a6	5949.05337	1394.93599
L	a7	-755.12572	189.73033
L	b0	25.4583	0.76014
L	b1	-58.16308	9.27284
L	b2	123.66296	24.59914
L	b3	-98.67771	22.59186
L	b4	26.18034	6.68298

Fig. S10 CO_2 virial fitting (lines) of the adsorption isotherms (points) of LIFM-WZ-3 measured at 273, 285 and 298 K.

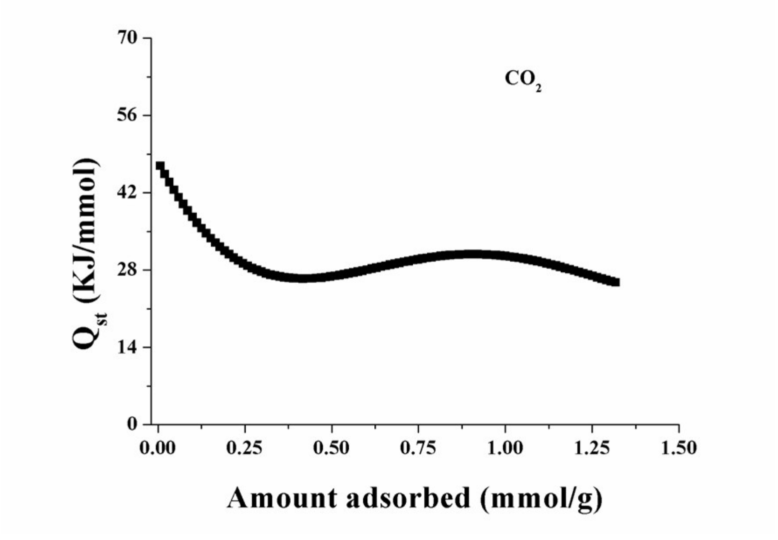

Fig. S11 CO_2 isosteric heat of LIFM-WZ-3.

6. CO_2/N_2, CO_2/CH_4, C_xH_y/CH_4, C_3/C_2 Selectivity Prediction via IAST

The experimental isotherm data for pure CO_2 and C_xH_y hydrocarbons (x = 1-3, measured at 273 K and 298 K) were fitted using a Langmuir Freundlich (LF) model:

$$q = \frac{a*b*p^{1/n}}{1+b*p^{1/n}}$$

Where q and p are adsorbed amounts and pressure of component i, respectively. The adsorption selectivities for binary mixtures of CO_2/N_2, CO_2/CH_4, C_xH_y/CH_4, were defined by

$$S_{i/j} = \frac{x_i}{x_j} * \frac{y_j}{yi}$$

were calculated using the Ideal Adsorption Solution Theory (IAST) of Myers and Prausnitz. Where x_i is the mole fraction of component i in the adsorbed phase and y_i is the mole fraction of component i in the bulk.

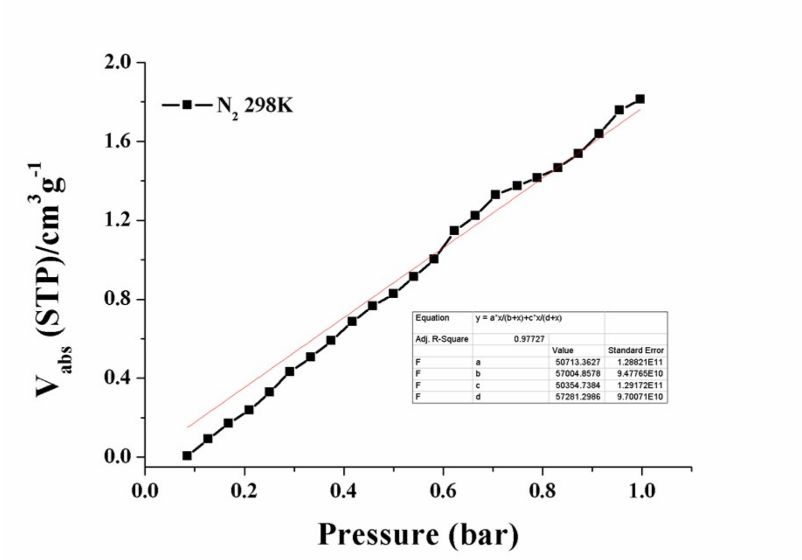

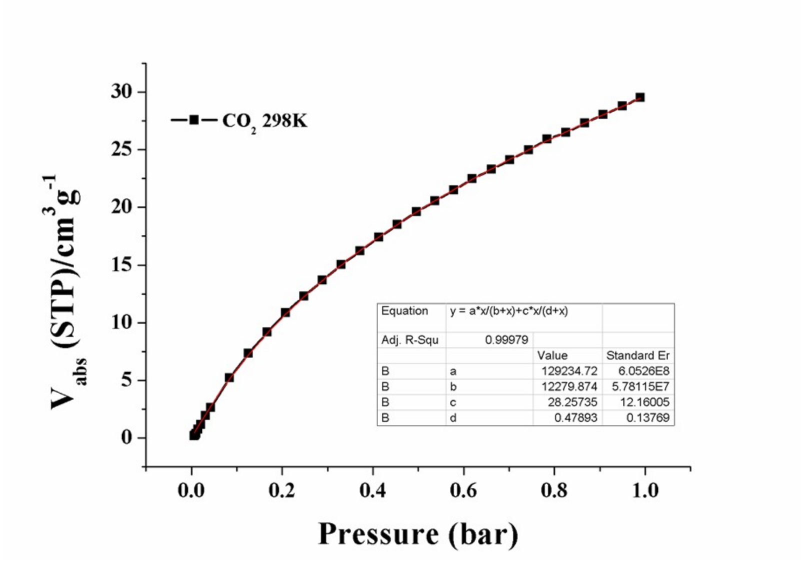

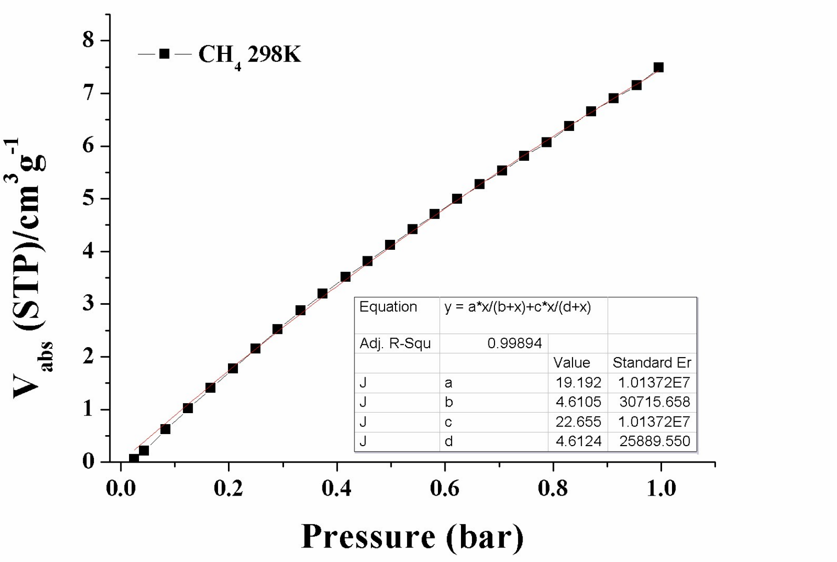

Equation	y = a*x/(b+x)+c*x/(d+x)		
Adj. R-Squ	0.99894		
		Value	Standard Er
J	a	19.192	1.01372E7
J	b	4.6105	30715.658
J	c	22.655	1.01372E7
J	d	4.6124	25889.550

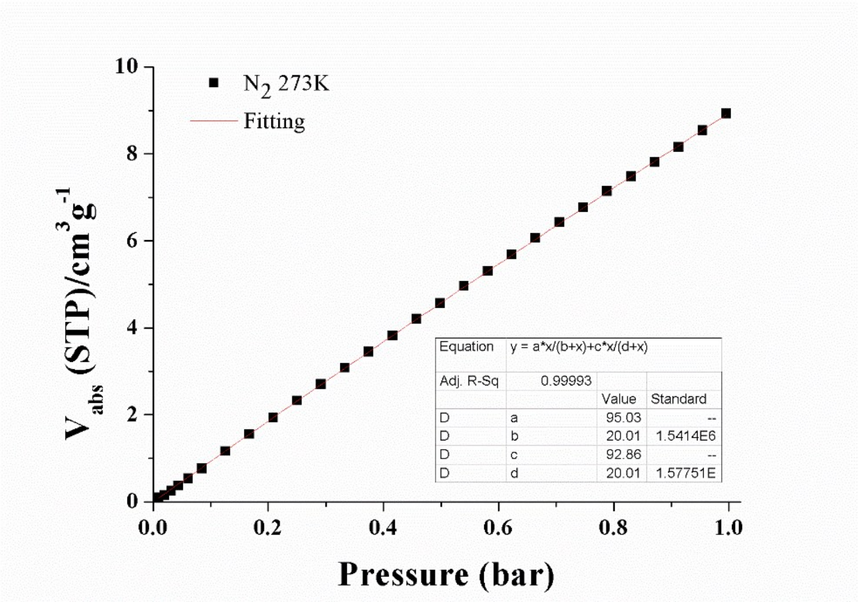

Equation	y = a*x/(b+x)+c*x/(d+x)		
Adj. R-Sq	0.99993		
		Value	Standard
D	a	95.03	--
D	b	20.01	1.5414E6
D	c	92.86	--
D	d	20.01	1.57751E

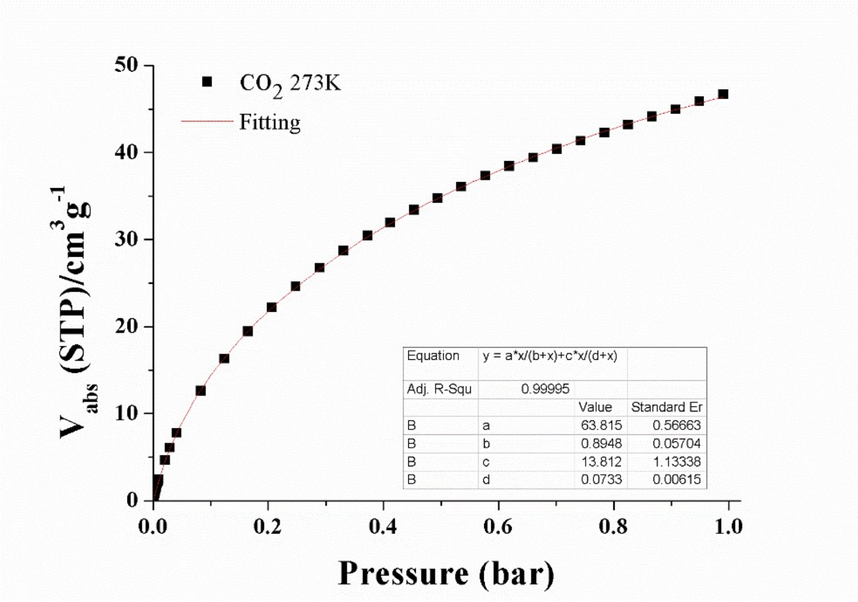

Equation	y = a*x/(b+x)+c*x/(d+x)		
Adj. R-Squ	0.99995		
		Value	Standard Er
B	a	63.815	0.56663
B	b	0.8948	0.05704
B	c	13.812	1.13338
B	d	0.0733	0.00615

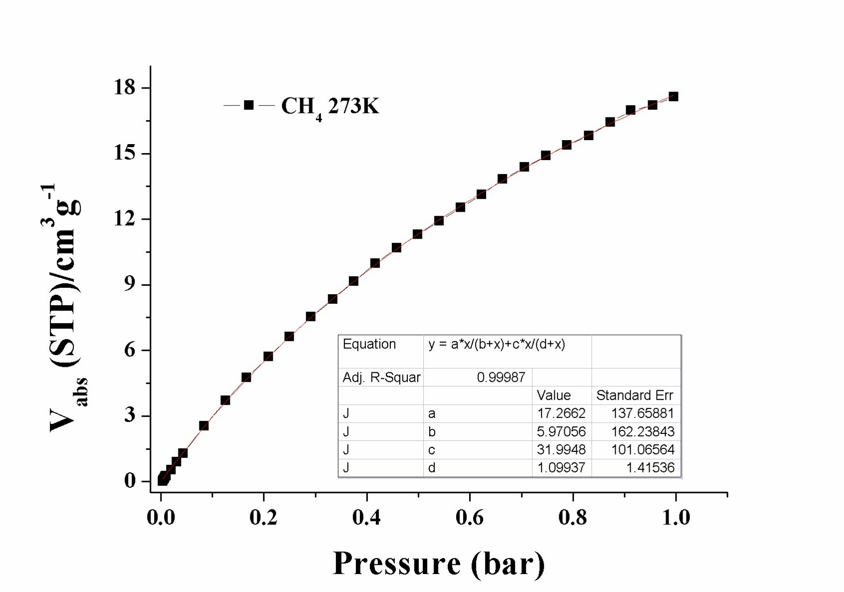

Equation	y = a*x/(b+x)+c*x/(d+x)		
Adj. R-Squar	0.99987		
		Value	Standard Err
J	a	17.2662	137.65881
J	b	5.97056	162.23843
J	c	31.9948	101.06564
J	d	1.09937	1.41536

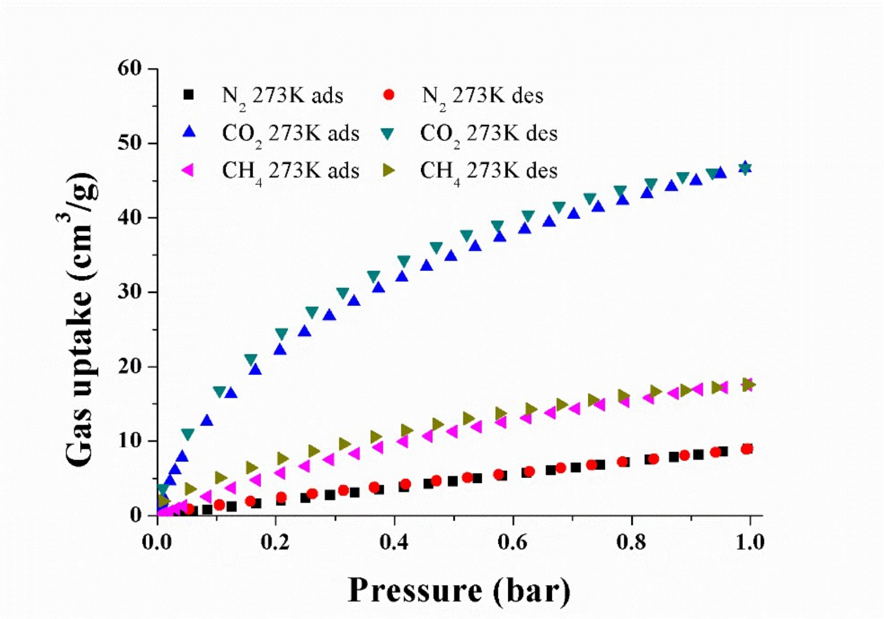

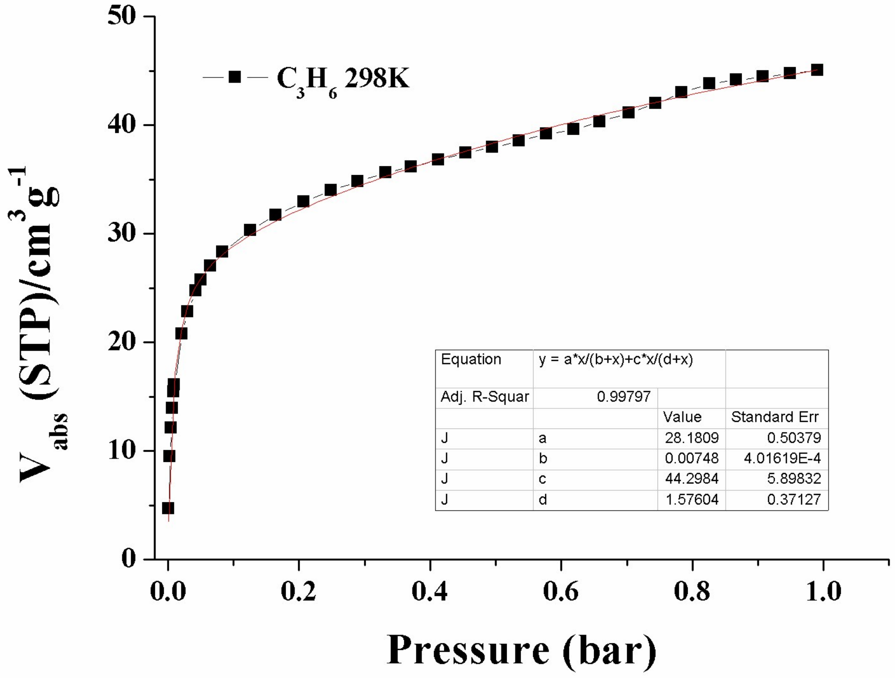

Equation	y = a*x/(b+x)+c*x/(d+x)		
Adj. R-Squar	0.99797		
		Value	Standard Err
J	a	28.1809	0.50379
J	b	0.00748	4.01619E-4
J	c	44.2984	5.89832
J	d	1.57604	0.37127

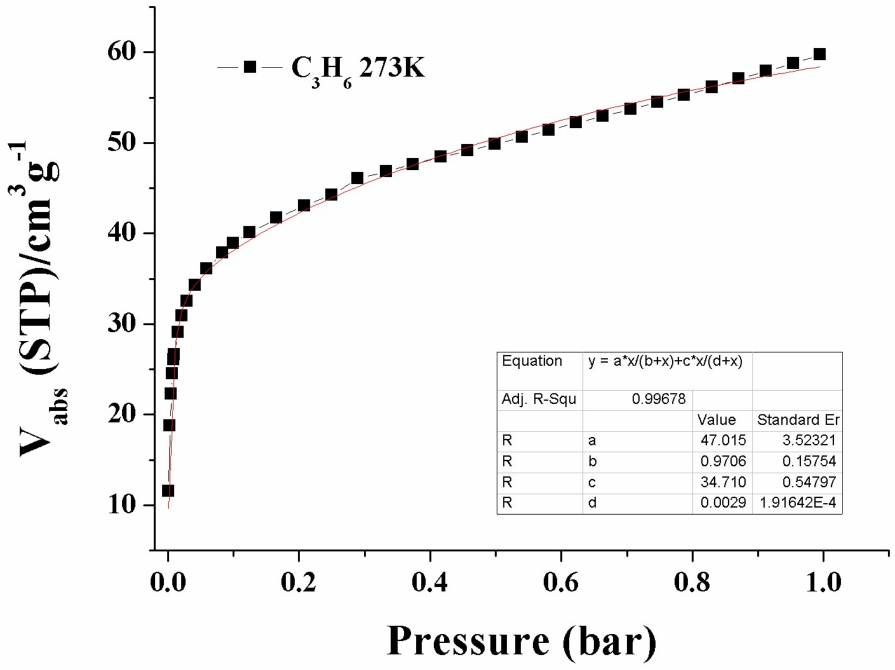

Equation	y = a*x/(b+x)+c*x/(d+x)		
Adj. R-Squ	0.99678		
		Value	Standard Er
R	a	47.015	3.52321
R	b	0.9706	0.15754
R	c	34.710	0.54797
R	d	0.0029	1.91642E-4

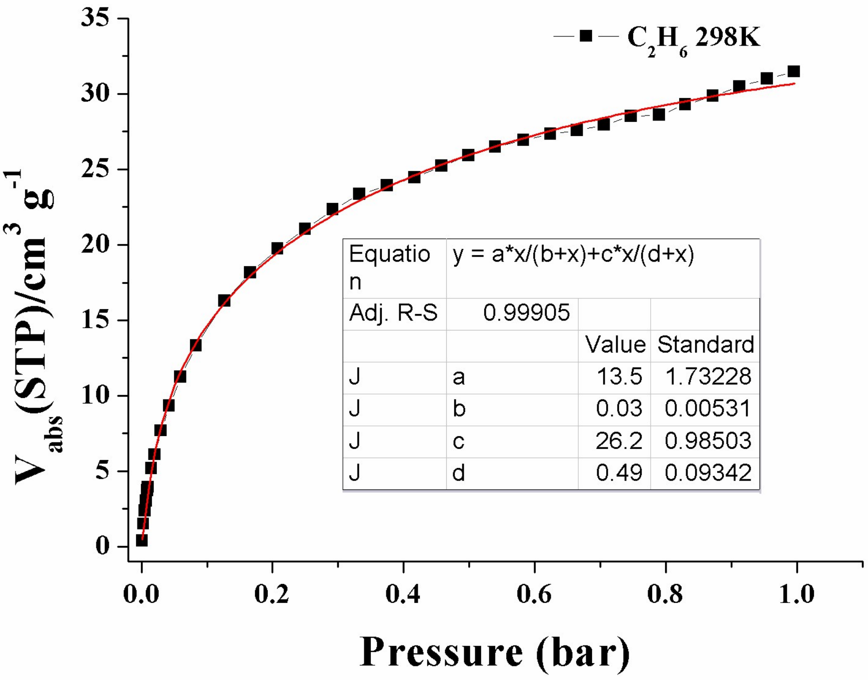

Equation	y = a*x/(b+x)+c*x/(d+x)		
Adj. R-S	0.99905		
		Value	Standard
J	a	13.5	1.73228
J	b	0.03	0.00531
J	c	26.2	0.98503
J	d	0.49	0.09342

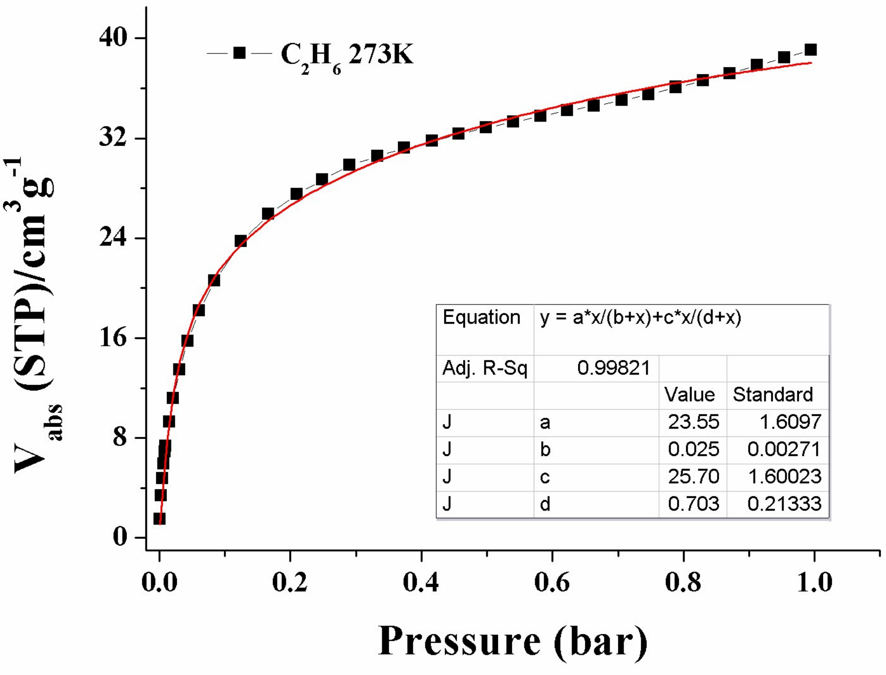

Equation	y = a*x/(b+x)+c*x/(d+x)		
Adj. R-Sq	0.99821		
		Value	Standard
J	a	23.55	1.6097
J	b	0.025	0.00271
J	c	25.70	1.60023
J	d	0.703	0.21333

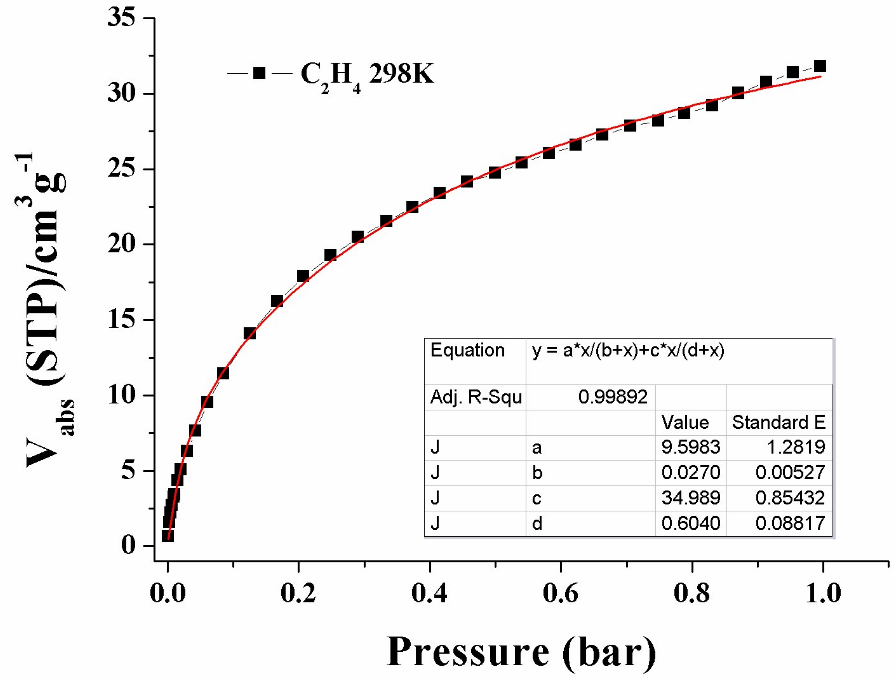

Equation	y = a*x/(b+x)+c*x/(d+x)		
Adj. R-Squ	0.99892		
		Value	Standard E
J	a	9.5983	1.2819
J	b	0.0270	0.00527
J	c	34.989	0.85432
J	d	0.6040	0.08817

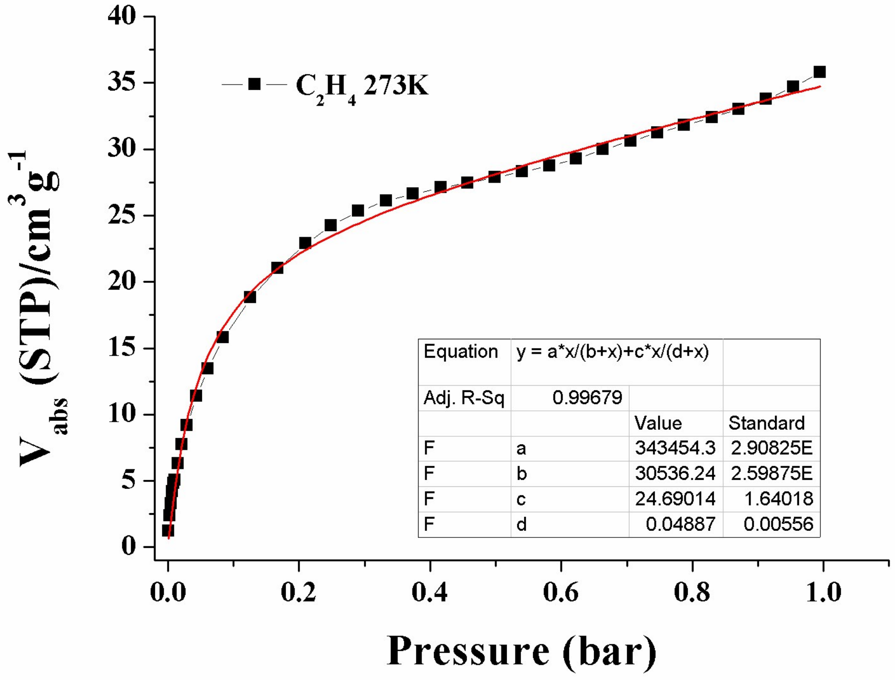

Equation	y = a*x/(b+x)+c*x/(d+x)		
Adj. R-Sq	0.99679		
		Value	Standard
F	a	343454.3	2.90825E
F	b	30536.24	2.59875E
F	c	24.69014	1.64018
F	d	0.04887	0.00556

Fig. S12 N_2, CO_2, CH_4, C_2H_4, C_2H_6 and C_3H_6 adsorption isotherms of LIFM-WZ-3 at 298 and 273 K fitted by LF model.

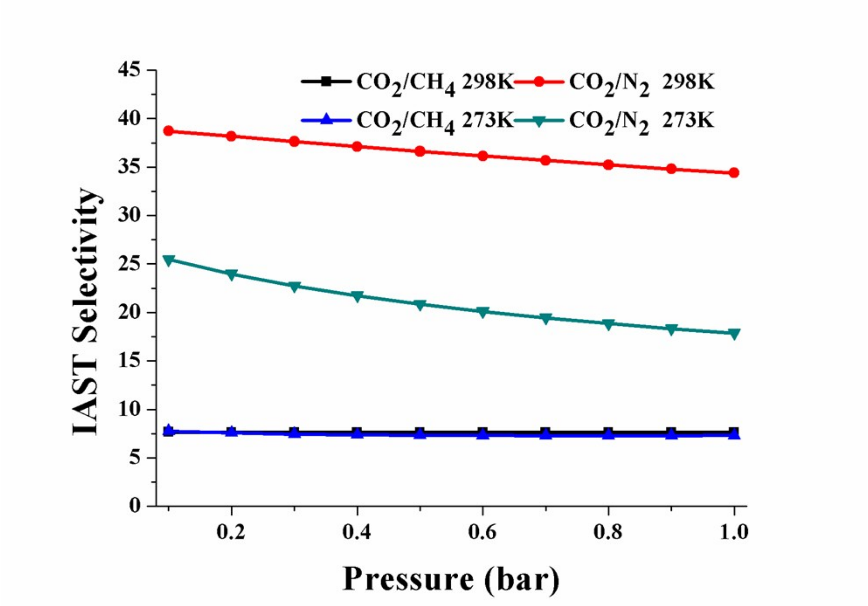

Fig. S13 Selectivities of CO_2/CH_4 (50:50) and CO_2/N_2 (15:85) at 298 and 273 K and calculated from the IAST based method.

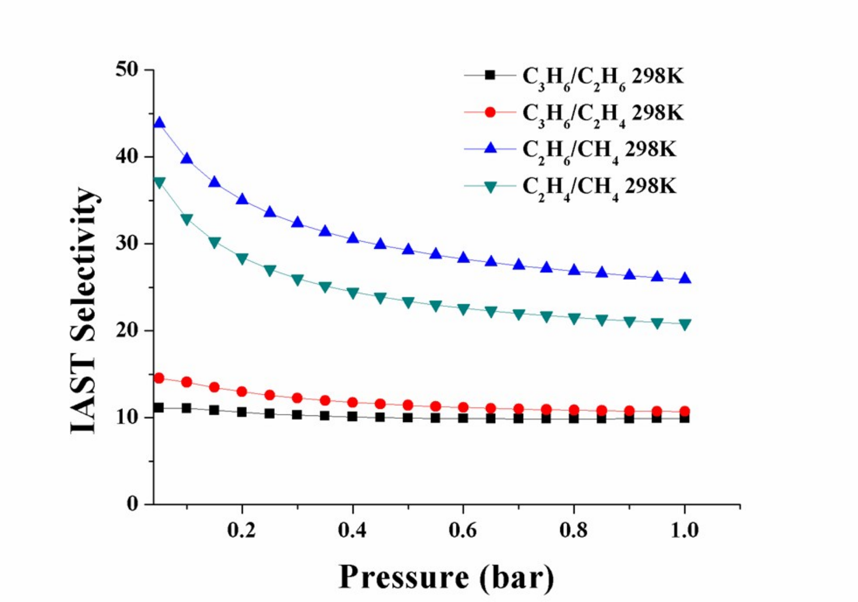

Fig. S14 Selectivities of C_3 hydrocarbon over C_2 and C_2 versus CH_4 (50:50) at 298 K and calculated from the IAST based method.

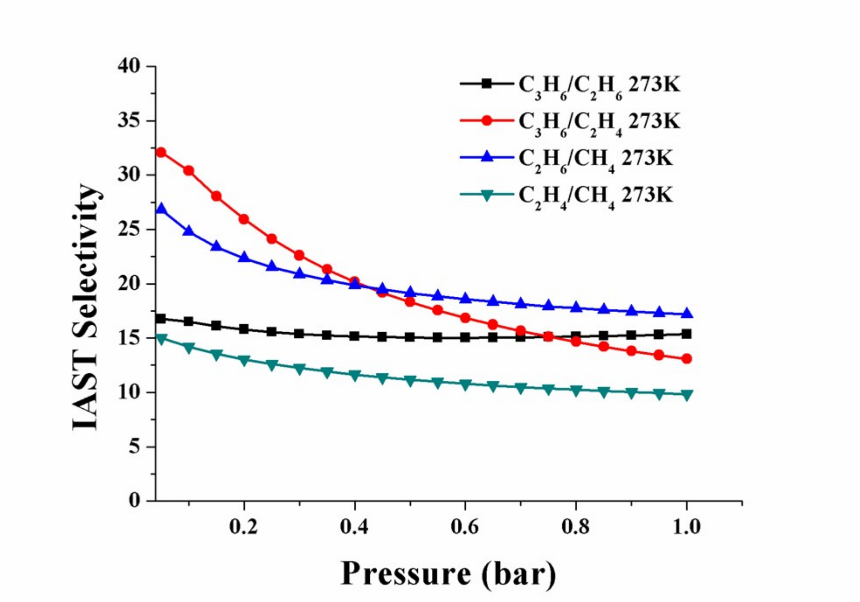

Fig. S15 Selectivities of C_3 hydrocarbon over C_2 and C_2 versus CH_4 (50:50) at 273 K and calculated from the IAST based method.

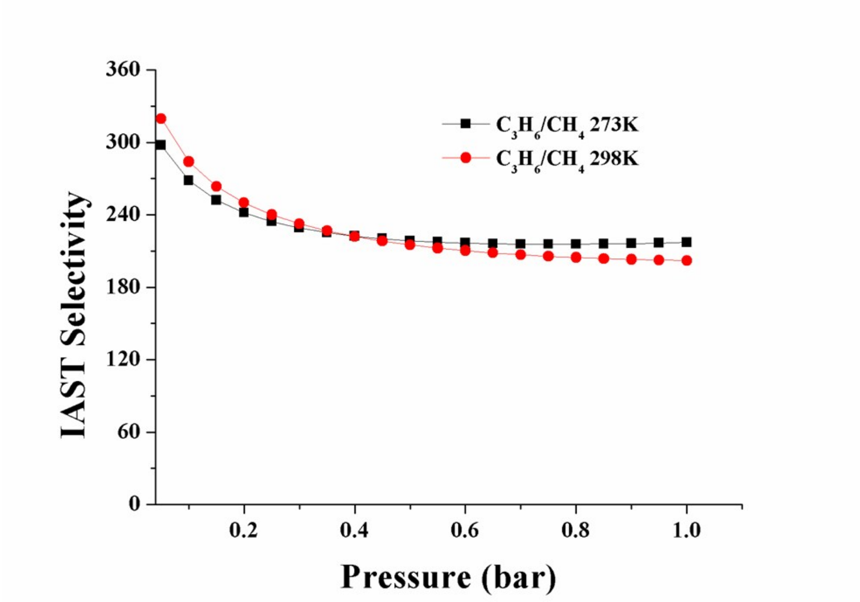

Fig. S16 Selectivities of C_3 over CH_4 (50:50) calculated from the IAST based method at 273 and 298 K.

7. More dye adsorption test results and photos

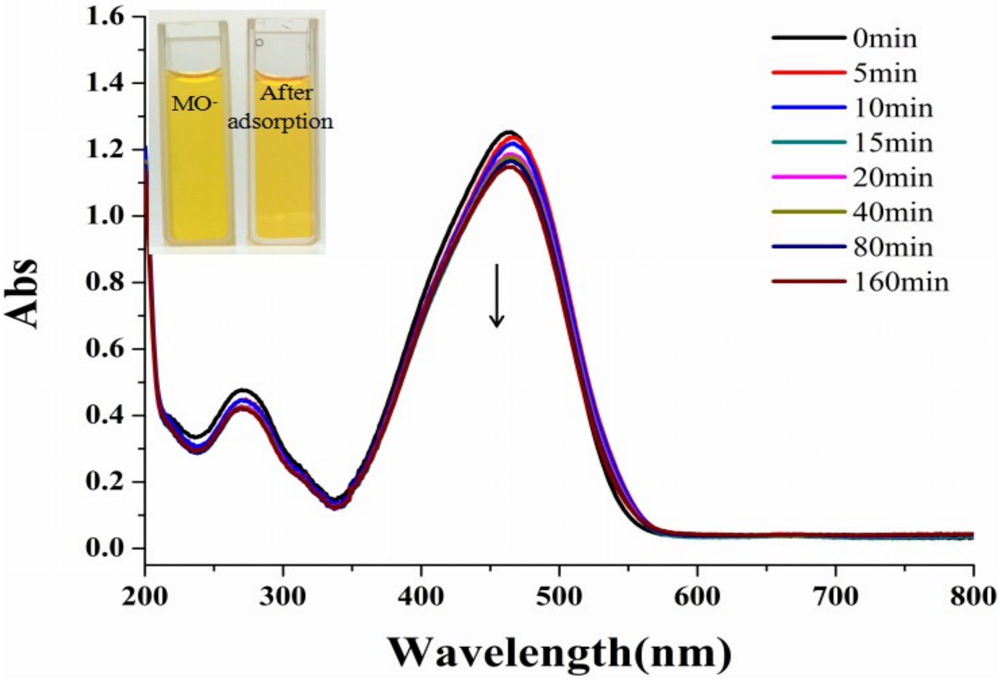

Fig. S17 Temporal evolution of UV-Vis absorption spectra of MO$^-$ in aqueous solution. The photographs show the colors of solution before and after 160 min of organic dye absorption.

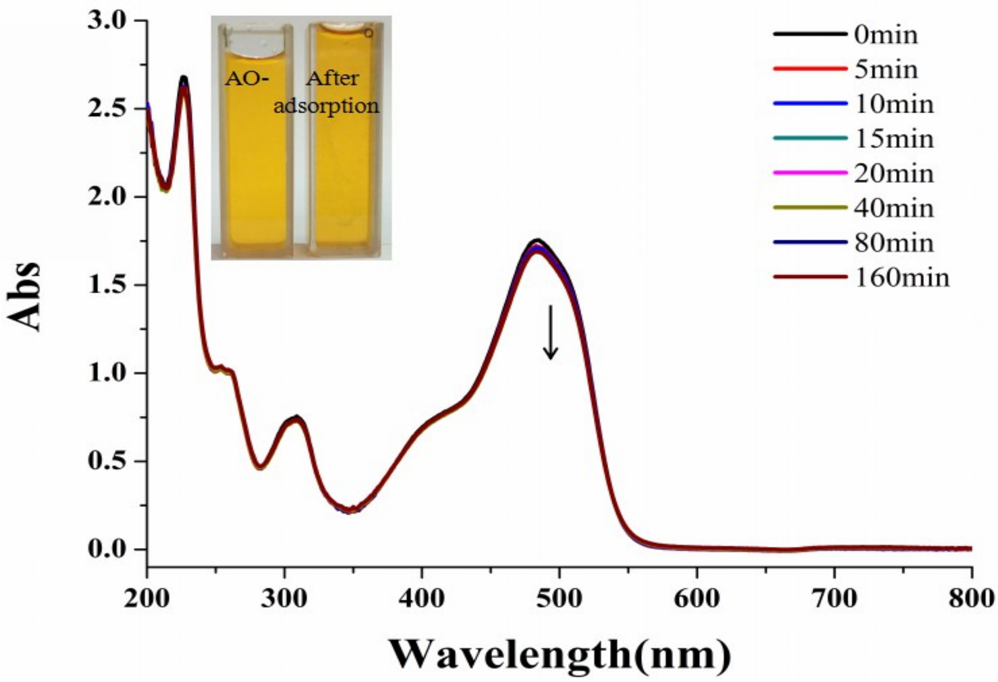

Fig. S18 Temporal evolution of UV-Vis absorption spectra of AO$^-$ in aqueous solution. The photographs show the colors of solution before and after 160 min of organic dye absorption.

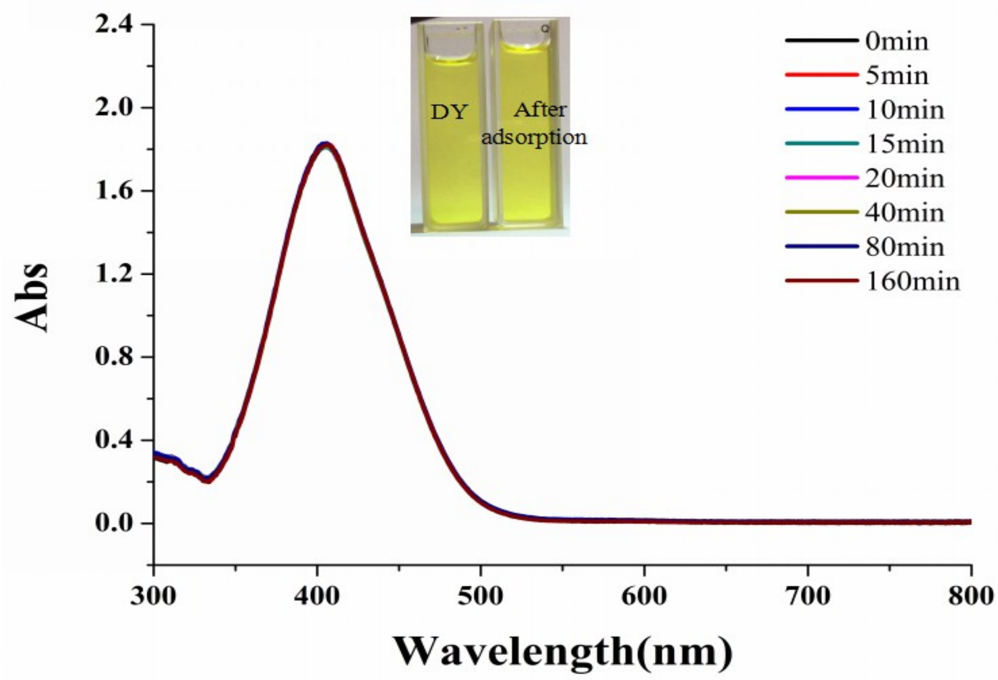

Fig. S19 Temporal evolution of UV-Vis absorption spectra of DY in aqueous solution. The photographs show the colors of solution before and after 160 min of organic dye absorption.

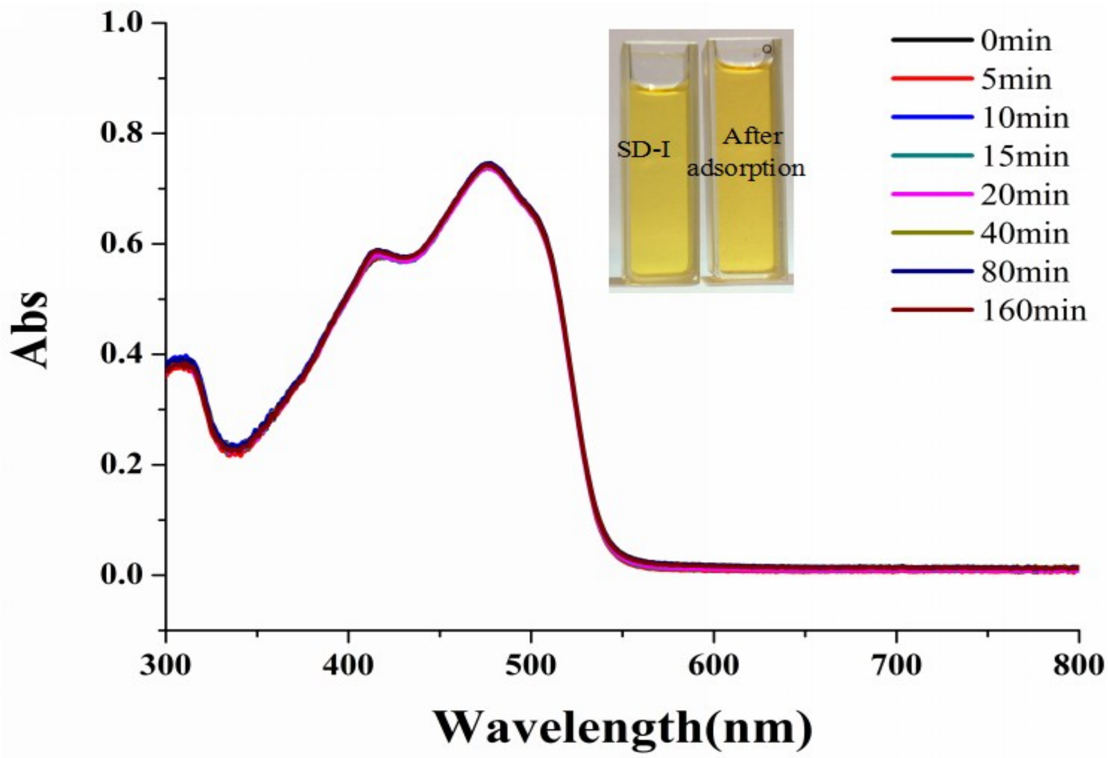

Fig. S20 Temporal evolution of UV-Vis absorption spectra of SD-I in aqueous solution. The photographs show the colors of solution before and after 160 min of organic dye absorption.

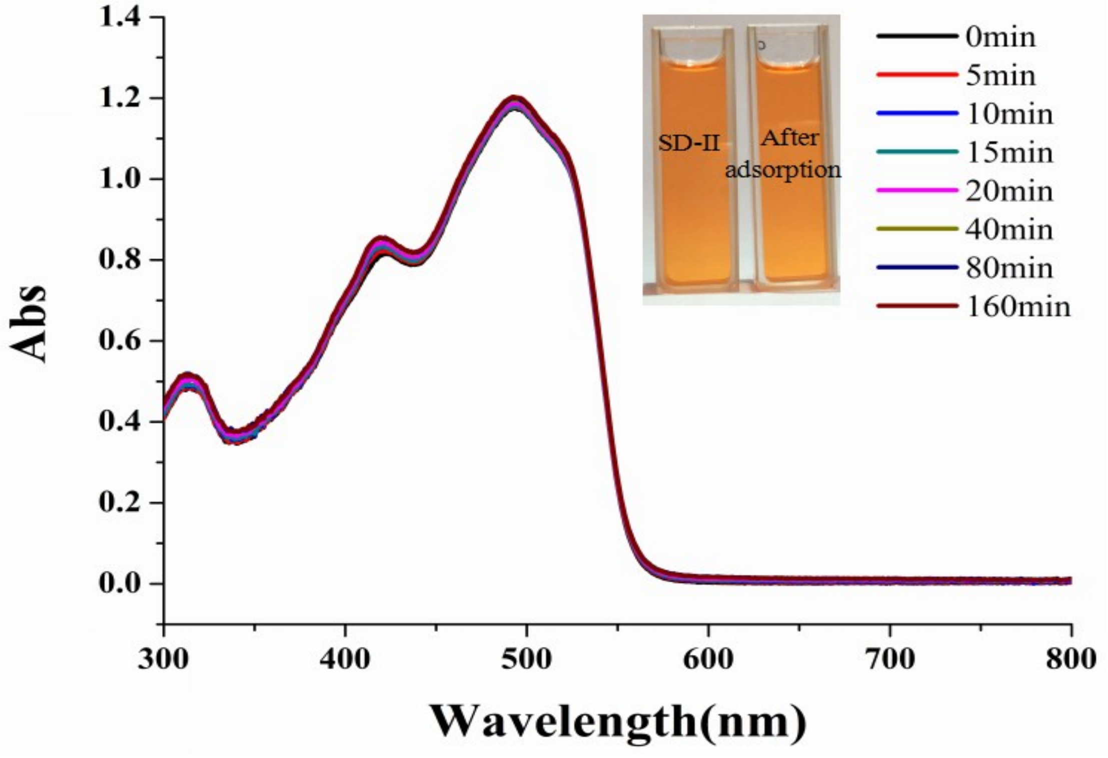

Fig. S21 Temporal evolution of UV-Vis absorption spectra of SD-II in aqueous solution. The photographs show the colors of solution before and after 160 min of organic dye absorption.

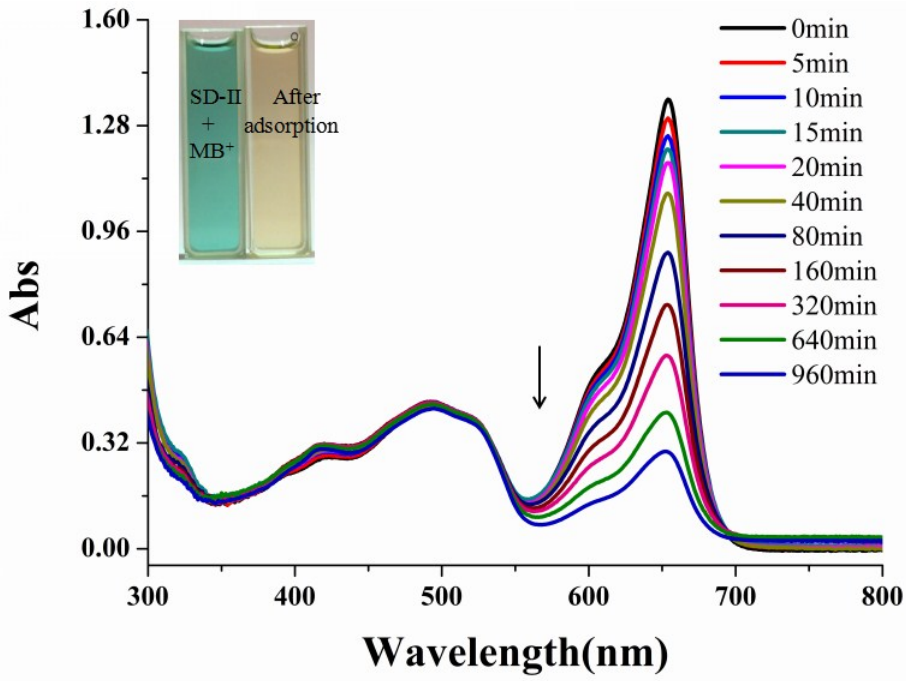

Fig. S22 Temporal evolution of UV-Vis absorption spectra of SD-II/MB$^+$ in aqueous solution. The photographs show the colors of solution before and after 960 min of organic dye absorption.

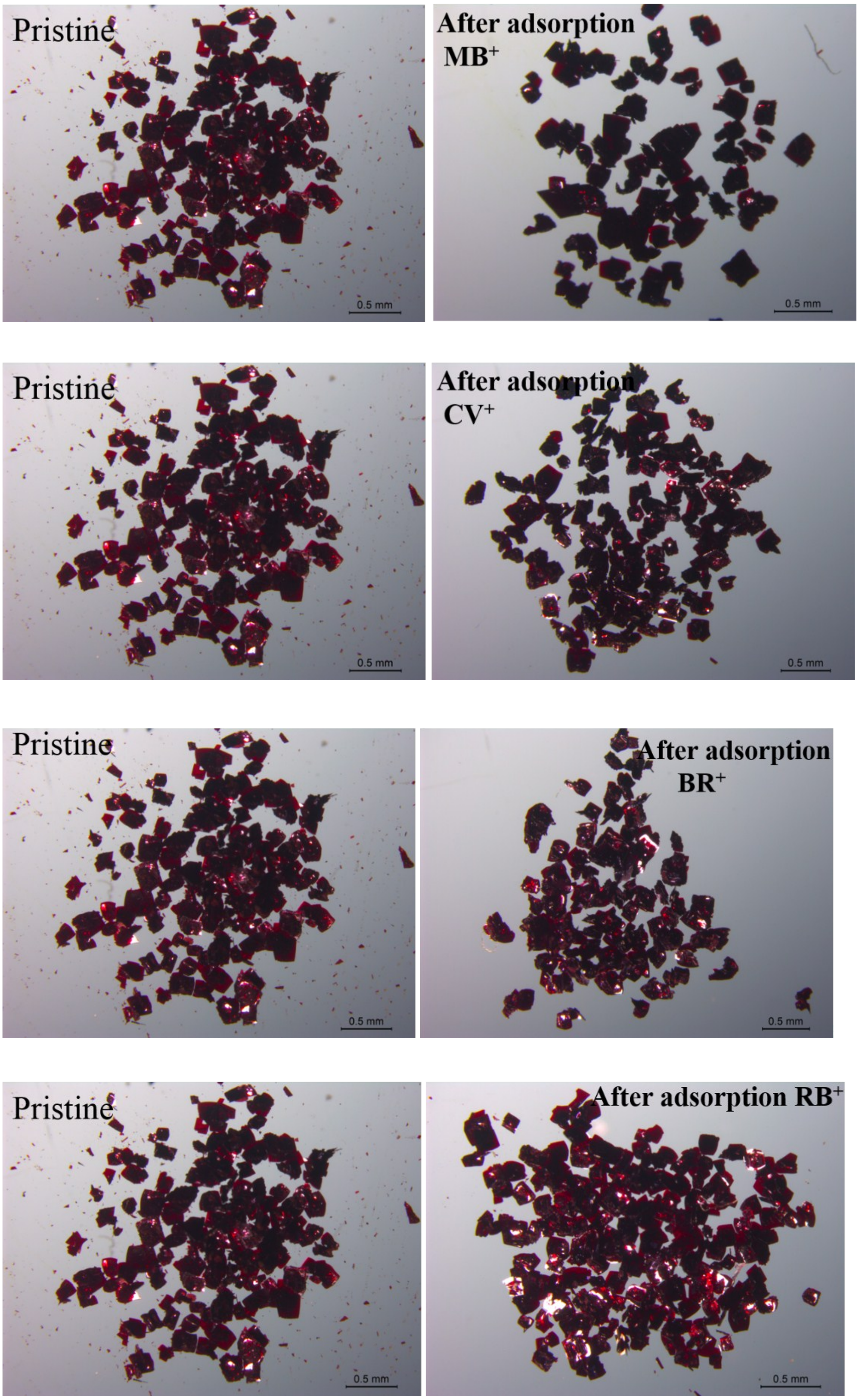

Fig. S23 The crystal photos of LIFM-WZ-3 before and after dye adsorption.

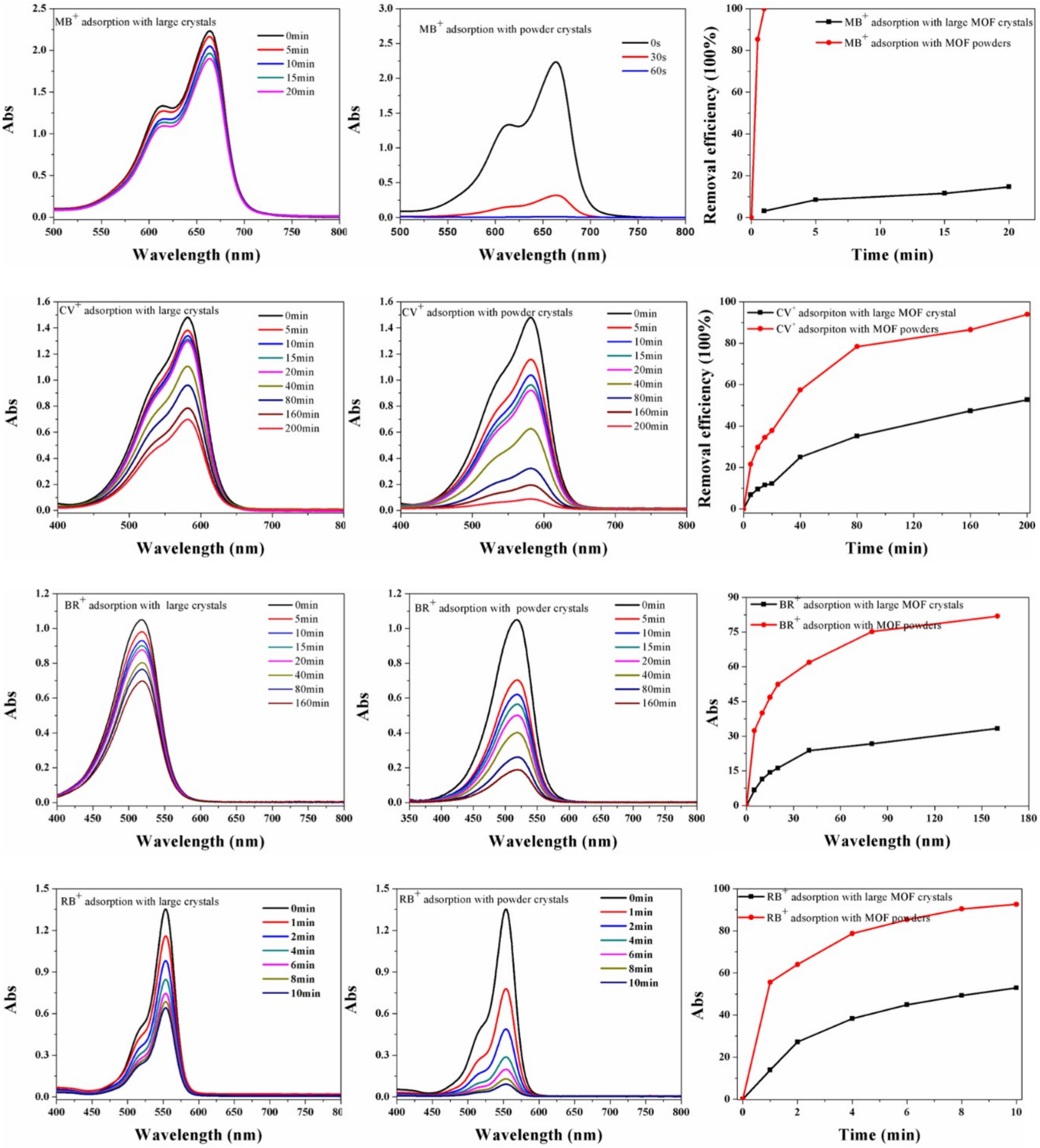

Fig. S24 Comparison between the dye adsorption and removal efficiency for MB^+, CV^+, BR^+ and RB^+ with LIFM-WZ-3 large crystals and powder samples, respectively (MB^+ for 20 mg L^{-1}, 20 ml; CV^+ for 20 mg L^{-1}, 20 ml; BR^+ for 20 mg L^{-1}, 20 ml; RB^+ for 5 mg L^{-1}, 20 ml).

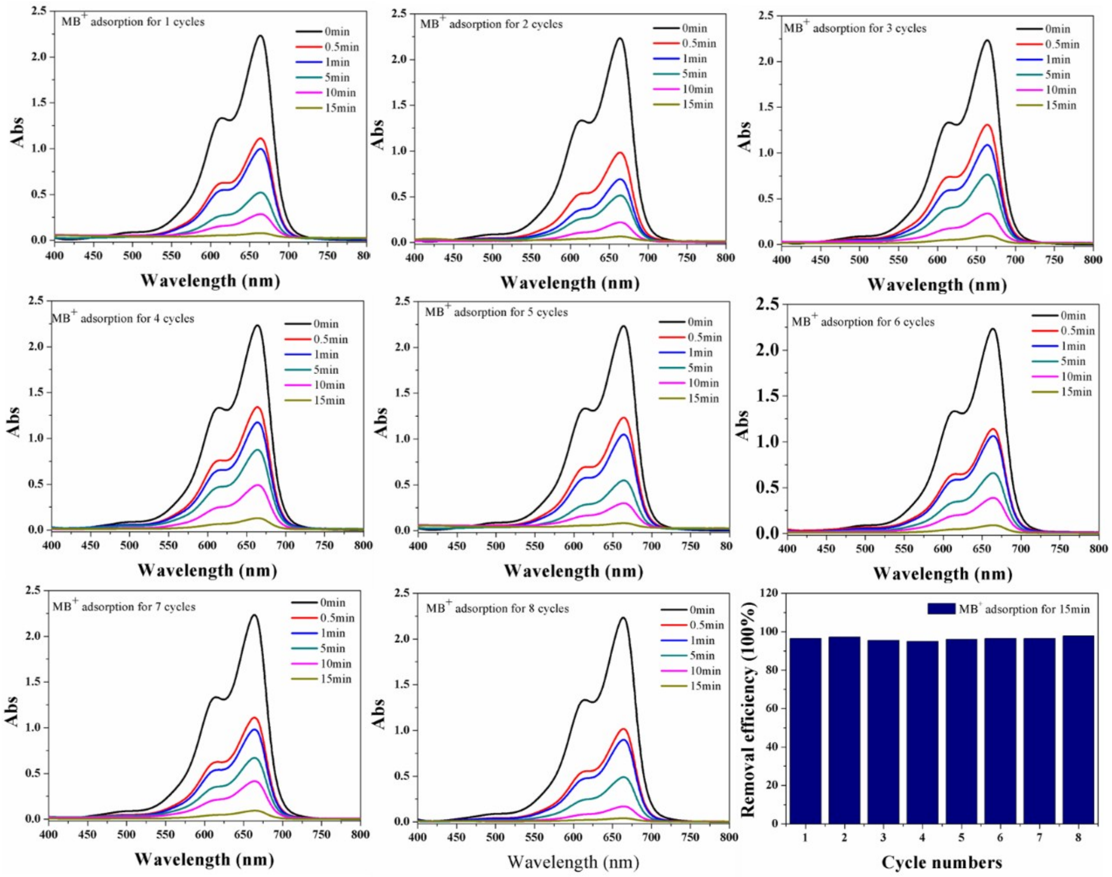

Fig. S25 Eight runs of recycling adsorption experiments of MB$^+$ by LIFM-WZ-3 (2 mg MOF powders in 20 ml aqueous solution with the MB$^+$ concentration of 20 mg L^{-1}).

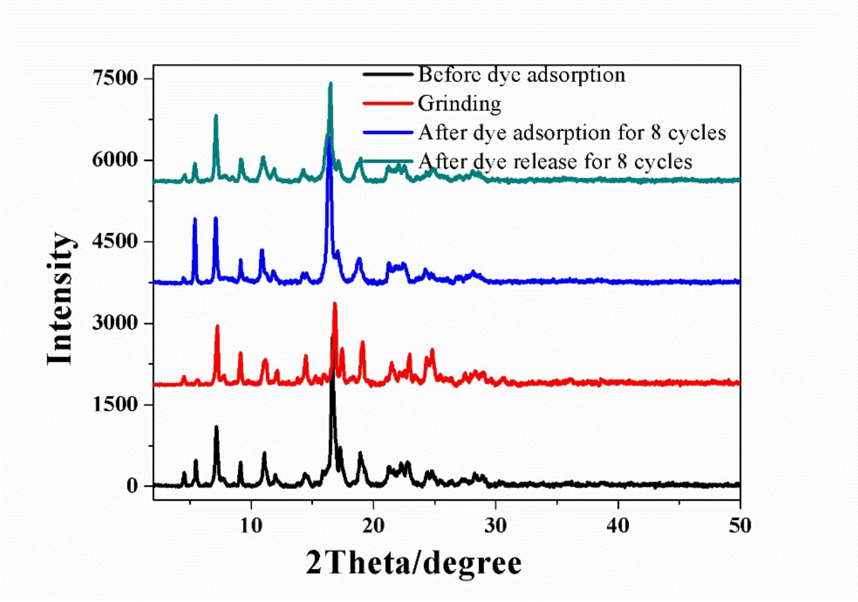

Fig. S26 PXRD patterns for LIFM-WZ-3 after repeated cycles of dye adsorption and release.

8. The adsorption capacity of LIFM-WZ-3 for different cationic dyes

The adsorption performance of LIFM-WZ-3 for MB^+, BR^+ and RB^+ was studied. Table S4 showed that the adsorbed capacities (q_t) of MB^+, CV^+ and RB^+ dyes on LIFM-WZ-3 related to time t, which can be calculated with the following relationship:

$$q_e = \frac{V(C_o - C_e)}{M}$$

$$q_t = \frac{V(C_o - C_t)}{M}$$

where q_e and q_t was the amount (mg/g) of dye adsorbed on the adsorbents at equilibrium and time t, respectively. C_0, C_e, and C_t were the liquid-phase concentrations (mg/L) of dye at initial, equilibrium, and time t, respectively. V (L) and M (g) were the volume (L) of the dye solutions and the mass of the adsorbents, respectively.

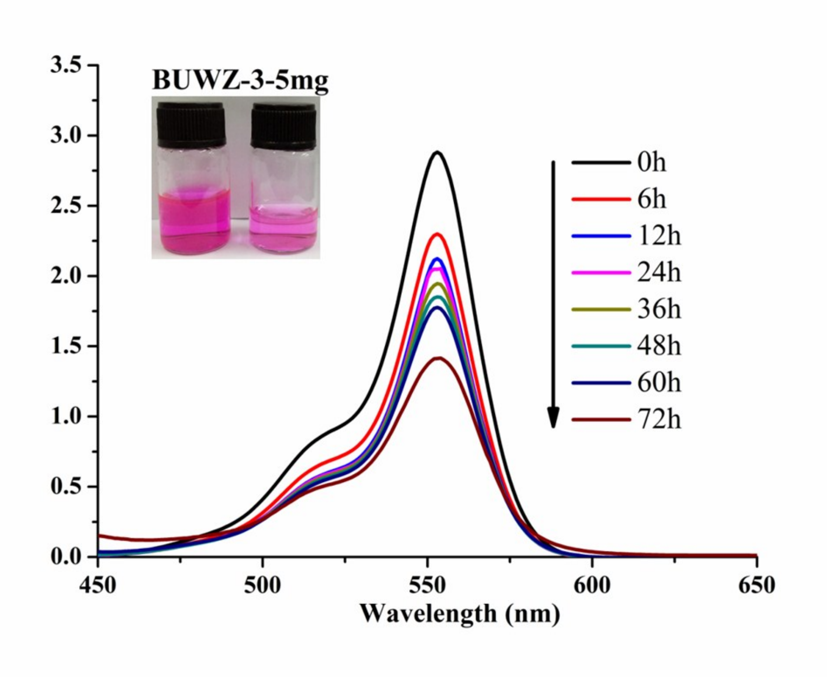

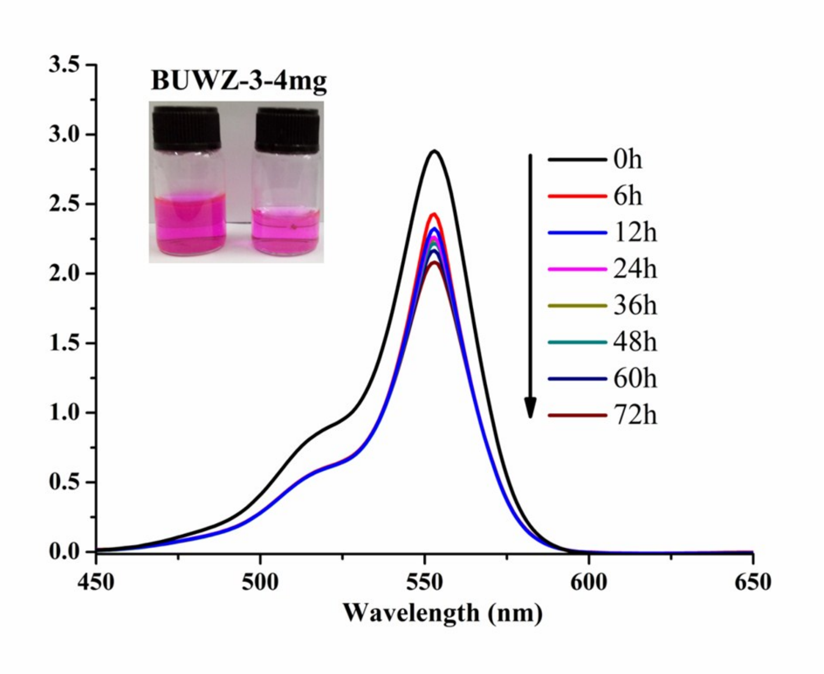
BUWZ-3-4mg
0.0
0.5
1.0
1.5
2.0
2.5
3.0
3.5
450
500
550
600
650
Wavelength (nm)
0h
6h
12h
24h
36h
48h
60h
72h

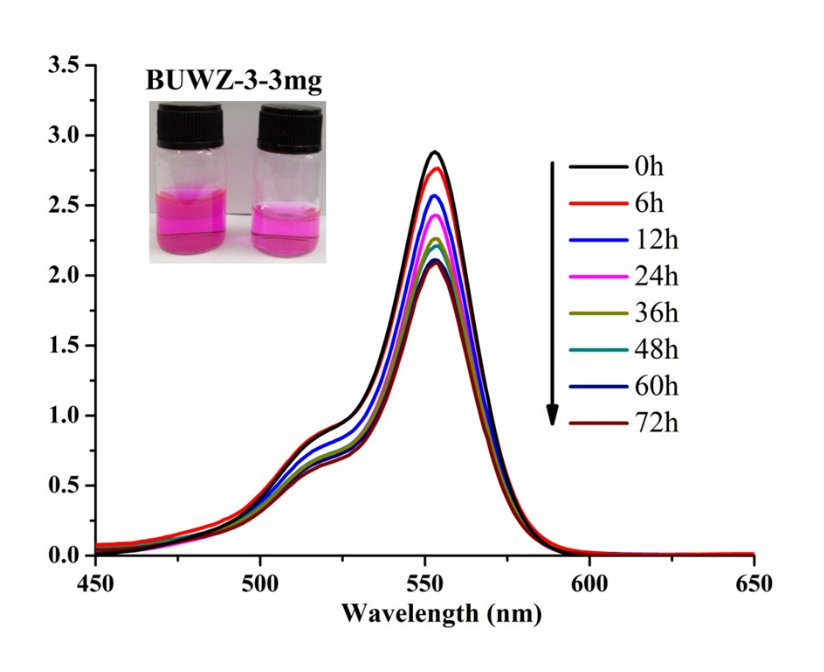
BUWZ-3-3mg
0.0
0.5
1.0
1.5
2.0
2.5
3.0
3.5
450
500
550
600
650
Wavelength (nm)
0h
6h
12h
24h
36h
48h
60h
72h

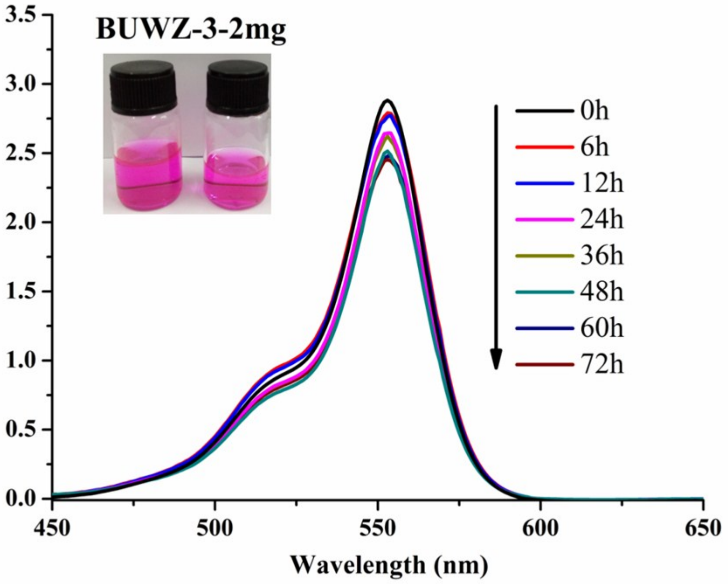

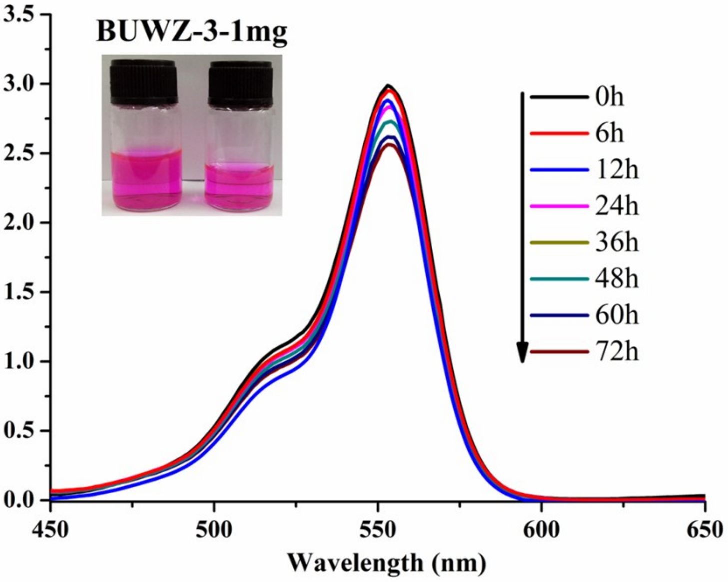

Fig. S27 Temporal evolution of UV-Vis absorption spectra of RB^+ in 20 ml aqueous solution (RB^+ for 20 mg/L) containing 1-5 mg LIFM-WZ-3, respectively. The photographs show the colors of solution before and after 72 h of organic dye absorption.

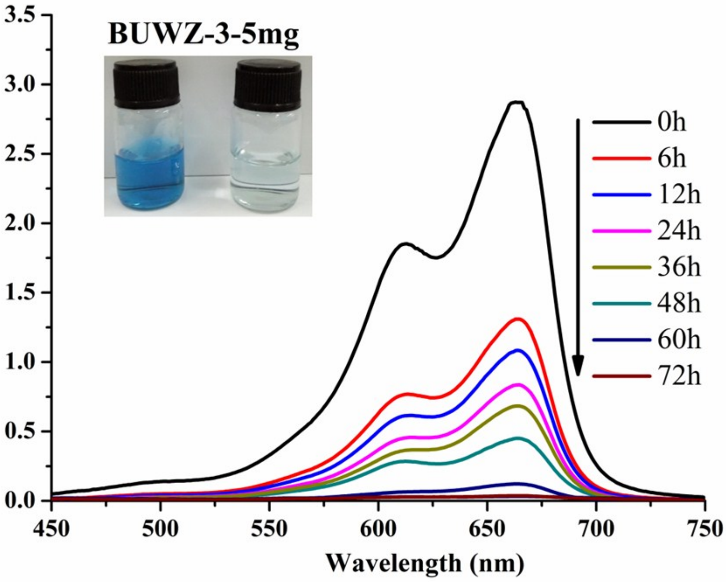
BUWZ-3-5mg
3.5
3.0
2.5
2.0
1.5
1.0
0.5
0.0
450
500
550
600
650
700
750
Wavelength (nm)
0h
6h
12h
24h
36h
48h
60h
72h

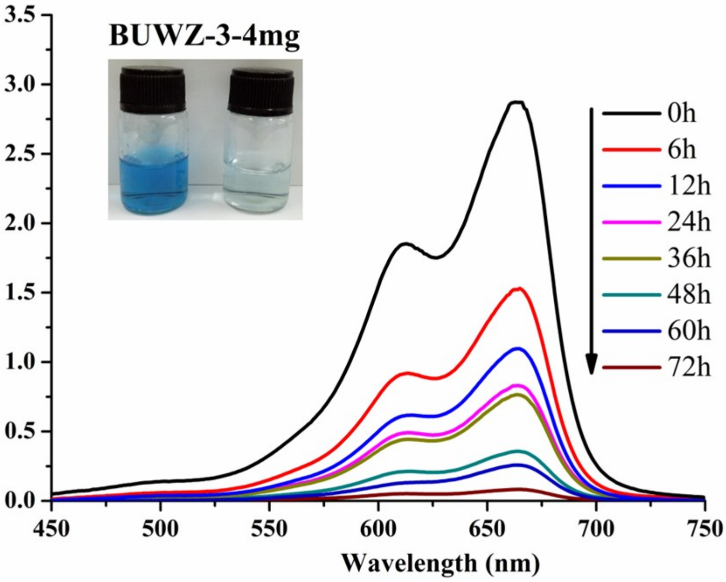
BUWZ-3-4mg
3.5
3.0
2.5
2.0
1.5
1.0
0.5
0.0
450
500
550
600
650
700
750
Wavelength (nm)
0h
6h
12h
24h
36h
48h
60h
72h

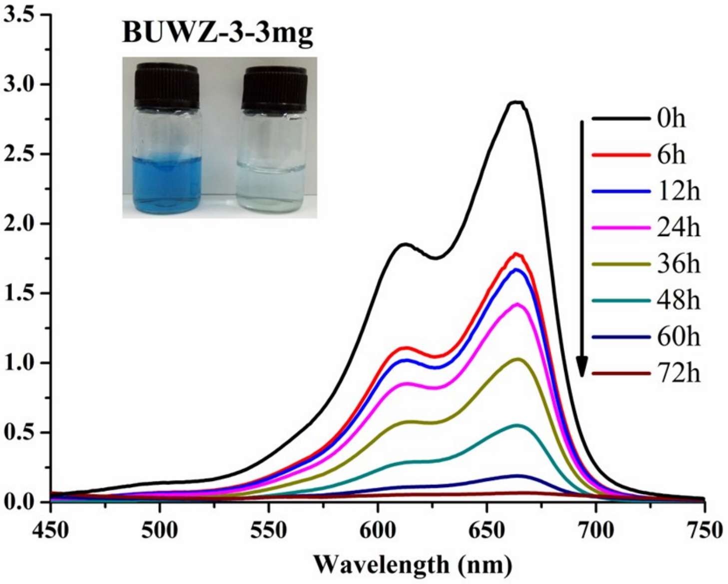
BUWZ-3-3mg
3.5
3.0
2.5
2.0
1.5
1.0
0.5
0.0
450
500
550
600
650
700
750
Wavelength (nm)
0h
6h
12h
24h
36h
48h
60h
72h

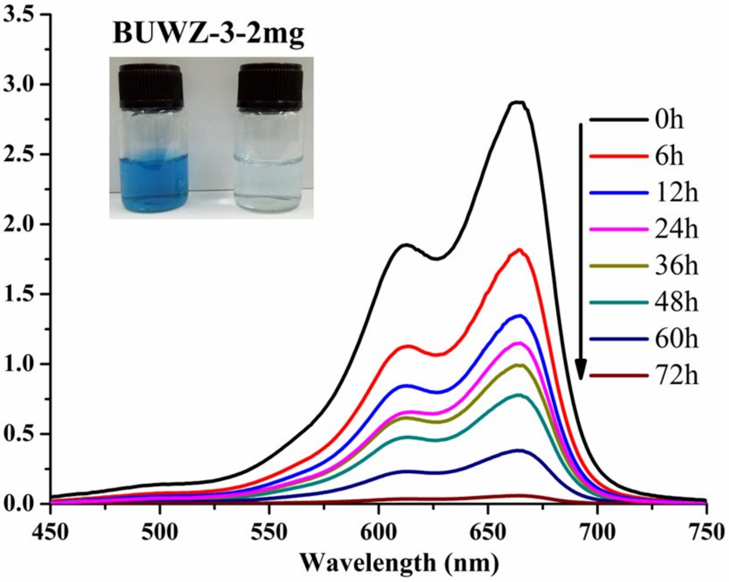
BUWZ-3-2mg
3.5
3.0
2.5
2.0
1.5
1.0
0.5
0.0
450
500
550
600
650
700
750
Wavelength (nm)
0h
6h
12h
24h
36h
48h
60h
72h

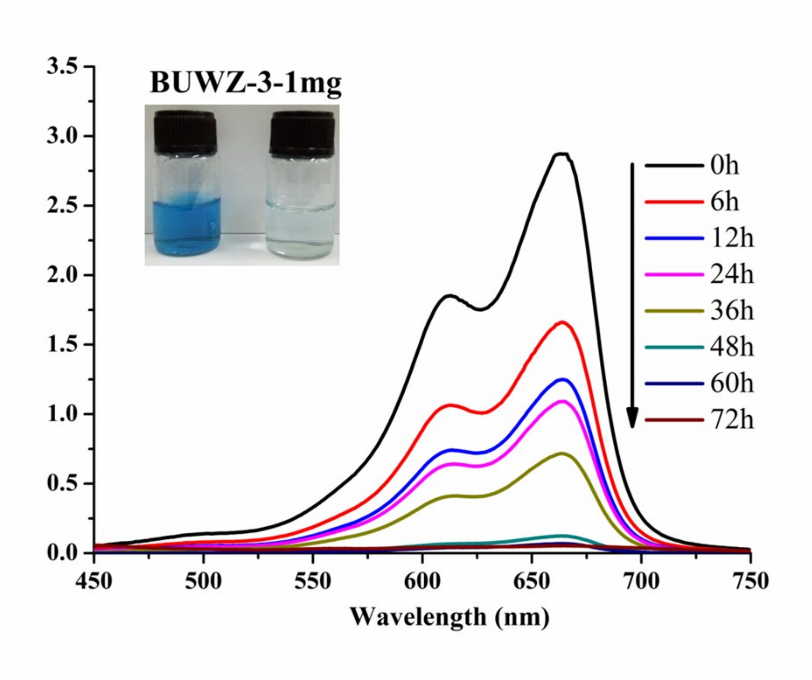

Fig. S28 Temporal evolution of UV-Vis absorption spectra of MB^+ in 20 ml aqueous solution (MB^+ for 20 mg/L) containing 1-5 mg LIFM-WZ-3, respectively. The photographs show the colors of solution before and after 72 h of organic dye absorption.

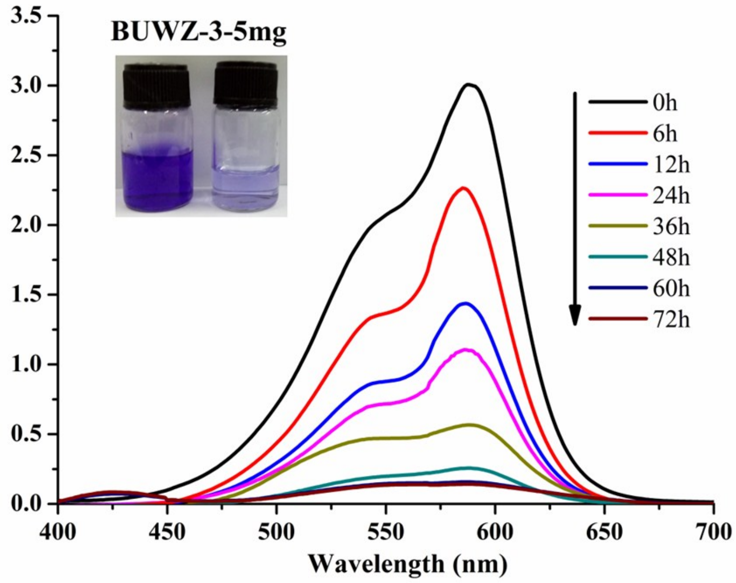
BUWZ-3-5mg
3.5
3.0
2.5
2.0
1.5
1.0
0.5
0.0
400
450
500
550
600
650
700
Wavelength (nm)
0h
6h
12h
24h
36h
48h
60h
72h

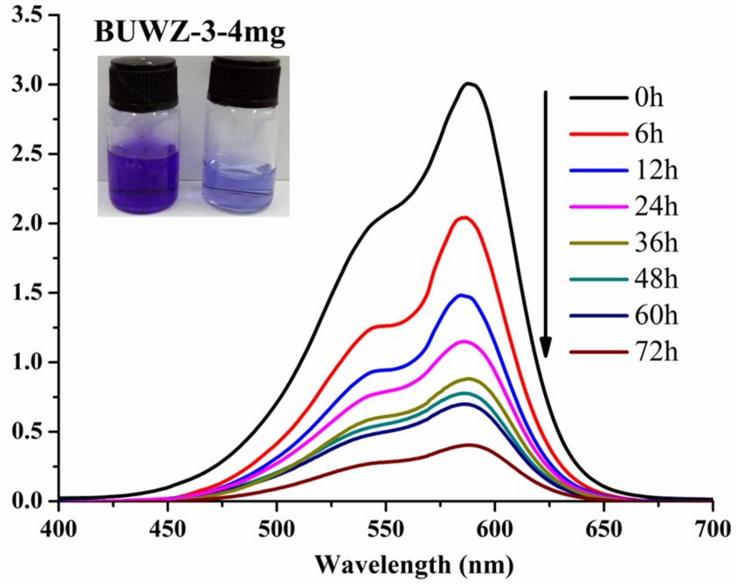
BUWZ-3-4mg
3.5
3.0
2.5
2.0
1.5
1.0
0.5
0.0
400
450
500
550
600
650
700
Wavelength (nm)
0h
6h
12h
24h
36h
48h
60h
72h

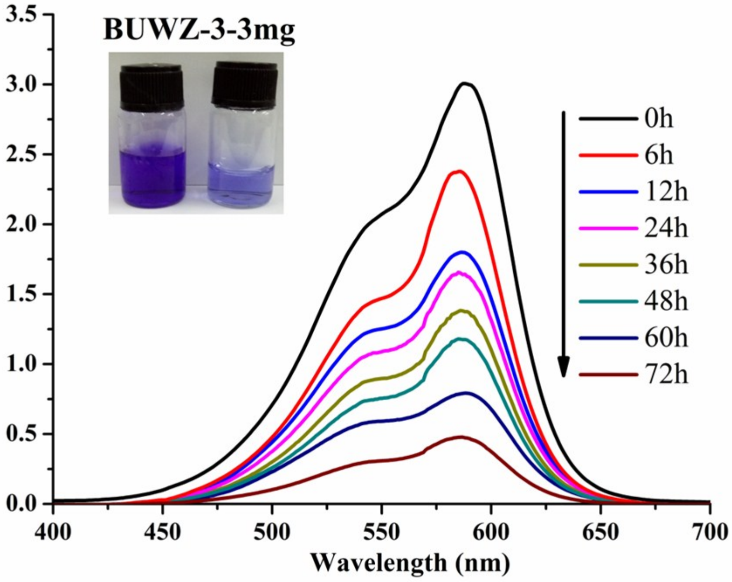
BUWZ-3-3mg
3.5
3.0
2.5
2.0
1.5
1.0
0.5
0.0
400
450
500
550
600
650
700
Wavelength (nm)
0h
6h
12h
24h
36h
48h
60h
72h

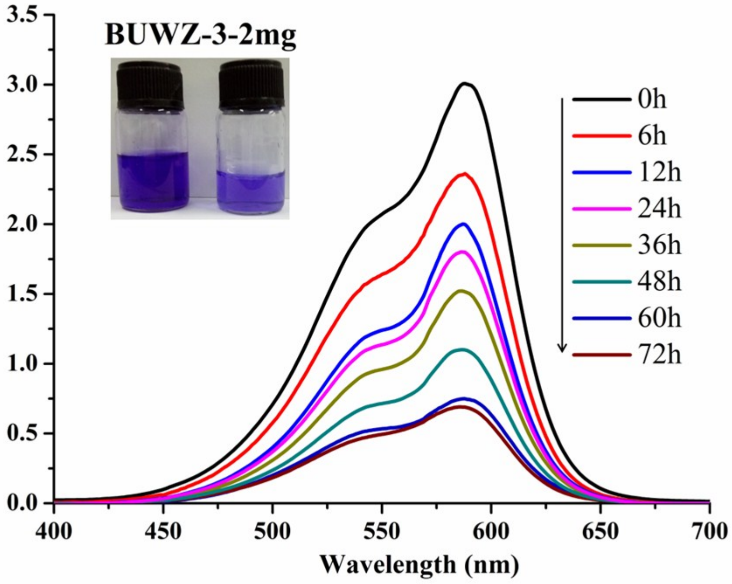
BUWZ-3-2mg
3.5
3.0
2.5
2.0
1.5
1.0
0.5
0.0
400
450
500
550
600
650
700
Wavelength (nm)
0h
6h
12h
24h
36h
48h
60h
72h

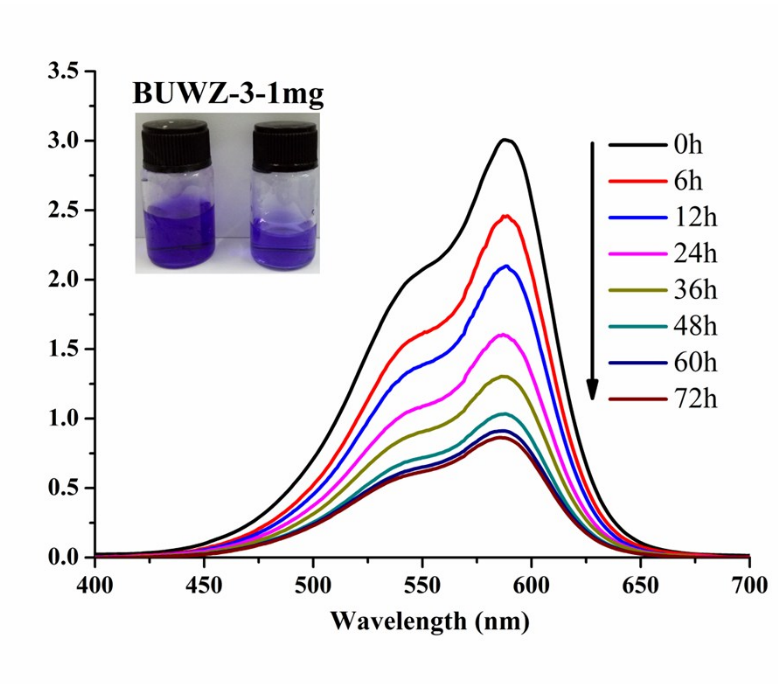

Fig. S29 Temporal evolution of UV-Vis absorption spectra of CV^+ in 20 ml aqueous solution (CV^+ for 20 mg/L) containing 1-5 mg LIFM-WZ-3, respectively. The photographs show the colors of solution before and after 72 h of organic dye absorption.

Table S4. The organic dye adsorption capacity of of 1-5 mg LIFM-WZ-3 after 72 h.

	Adsorption capacity (mg g^{-1})		
Amounts of adsorbent	MB^+	CV^+	RB^+
5 mg	197.2	189.7	105.1
4 mg	242.19	217.5	76.6
3 mg	324	282.3	101.67
2 mg	489.25	383.25	91
1 mg	983	713.5	141.5